Adaptation and coordinated evolution of plant hydraulic traits

TITLE: Adaptation and coordinated evolution of plant hydraulic traits.

Pablo Sanchez-Martinez, Jordi Martínez-Vilalta, Kyle G. Dexter, Ricardo A. Segovia and Maurizio Mencuccini

Affiliations and emails:

Pablo Sanchez Martinez[1,2]: Email: p.sanchez@creaf.uab.cat Affiliations: (1) CREAF,Cerdanyola del Valles, 08193 Barcelona, Spain; (2) Universitat Autònoma de Barcelona, Cerdanyola del Valles, 08193 Barcelona, Spain

Jordi Martínez-Vilalta[1,2]: Email: Jordi.Martinez.Vilalta@uab.cat Affiliations: (1) CREAF, Cerdanyola del Valles, 08193 Barcelona, Spain (2) Universitat Autònoma de Barcelona, Cerdanyola del Valles, 08193 Barcelona, Spain

Kyle G. Dexter[3,4]: Email: Kyle.Dexter@ed.ac.uk Affiliations: (3) School of GeoSciences, University of Edinburgh, Edinburgh, United Kingdom (4) Royal Botanic Garden Edinburgh, Edinburgh, United Kingdom

Ricardo A. Segovia[3,5]: Email: segovia@ug.uchile.cl Affiliations: (3) School of GeoSciences, University of Edinburgh, Edinburgh, United Kingdom (5) Instituto de Ecología y Biodiversidad (www.ieb chile.cl), Santiago, Chile

Maurizio Mencuccini[1,6]: Email: m.mencuccini@creaf.uab.cat Affiliations: (1) CREAF, Cerdanyola del Valles, 08193 Barcelona, Spain (6) ICREA, Pg. Lluís Companys 23, 08010, Barcelona, Spain

Running title: **hydraulic traits evolution**

Keywords: global, plant hydraulics, evolution, phylogenetic comparative methods, phylogenetic mixed models, adaptation, phylogenetic conservatism, evolutionary correlation.

Corresponding Author: Pablo Sanchez-Martinez: p.sanchez@creaf.uab.cat, Carrer Sant Martí de Porres 1-3, 2-4, 08032 Barcelona, Spain. Telephone: +34 644376756. ORCID ID: https://orcid.org/0000-0002-0157-7800.

1   **Abstract**

2   Hydraulic properties control plant responses to climate and are likely to be under strong selective

3   pressure, but their macro-evolutionary history remains poorly characterized. To fill this gap, we

4   compiled a global dataset of hydraulic traits describing xylem conductivity (K_s), xylem resistance

5   to embolism (P50), sapwood allocation relative to leaf area (Hv) and drought exposure (ψ_{min}), and

6   matched it with global seed plant phylogenies. Individually, these traits present medium to high

7   levels of phylogenetic signal, partly related to environmental selective pressures shaping lineage

8   evolution. Most of these traits evolved independently of each other, being co-selected by the same

9   environmental pressures. However, the evolutionary correlations between P50 and ψ_{min} and

10   between K_s and Hv show signs of deeper evolutionary integration because of functional,

11   developmental or genetic constraints, conforming to evolutionary modules. We do not detect

12   evolutionary integration between conductivity and resistance to embolism, rejecting a hardwired

13   trade-off for this pair of traits.

Introduction

Water transport in plants occurs under negative pressure and is driven by the process of transpiration at the leaf-atmosphere interface, which generates a water potential gradient throughout the plant (cohesion-tension theory) (Dixon 1914). A key source of vulnerability for the water transport system is the formation of xylem embolism, resulting from the breakage of the water columns caused by cavitation (the phase change from liquid water to gas), which reduces hydraulic conductivity and may lead to plant death through hydraulic failure (Tyree & Zimmermann 2002). This process is more likely to occur during drought events, as low water availability results in low soil plant water potentials, and becomes more pronounced also with high temperatures, which provoke an increase in atmospheric evaporative demand (Venturas *et al.* 2017). A wealth of research over the last decades has established that hydraulic failure is a principal mechanism triggering tree mortality under drought (Adams *et al.* 2017). Therefore, drought and high temperatures, together with other important sources of selection such as freezing temperatures (Zanne *et al.* 2014), have been considered among the primary forces shaping plant evolution by acting directly on hydraulic traits (Maherali *et al.* 2004). However, global patterns in the evolution of hydraulic traits remain only partly characterized and their relationship with relevant environmental selective pressures poorly identified.

Species differ greatly in their exposure to low water potentials and in their capacity to operate under such conditions. The actual hydraulic risk is normally represented by the hydraulic safety margin (HSM) (Choat *et al.* 2012). HSM integrates both drought stress exposure at the tissue level, measured as the minimum leaf water potential registered for a given species (ψ_{min}), and resistance to embolism, quantified as the water potential that causes a 50% reduction in stem hydraulic conductivity (P50) (HSM = ψ_{min} - P50). Plants with low (or even negative) safety margins

4

experience large amounts of embolism (Choat *et al.* 2012, 2018). ψ_{min} emerges from the balance

between soil water availability, the rate of water loss, and the capacity of the plant transport system

to supply water to leaves, and it is thus determined by plant functional properties such as rooting

strategy, leaf phenology and stomatal control as well as by abiotic factors such as soil water

availability and atmospheric evaporative demand (Bhaskar & Ackerly 2006). Meanwhile, P50 is

primarily explained by xylem anatomical features (Venturas *et al.* 2017). P50 and ψ_{min} are known

to co-vary, leading to relatively invariant HSMs at the global scale and to respond to similar

environmental selective pressures related to water availability (Choat *et al.* 2012). For instance,

stem P50 has been reported to be negatively related with precipitation for 10 conifer species from

different habitats (Brodribb & Hill 1999) and for the gymnosperm genus *Callitris* (Larter *et al.*

2017) and ψ_{min} has been positively related to variables determining water availability (Bhaskar &

Ackerly 2006) and negatively to soil particle size during drought for Great Basin shrubs (Sperry

& Hacke 2002). Since the risk of hydraulic failure is likely to be under greater selective pressure

than ψ_{min} and P50 *per se*, these two latter traits are expected to be integrated over the evolutionary

history of lineages, specifically meaning that they evolve in a coordinated fashion (i.e., non-

independently from each other), representing an evolutionary module.

Xylem conductive capacity is another key determinant of hydraulic function, usually quantified as

the maximum, stem-specific hydraulic conductivity (K_s). This property has been reported to be

positively related to temperature and precipitation at a global scale (He *et al.* 2020). Because the

structural properties of xylem conduits and pit membranes associated with increased embolism

resistance (quantified here as P50) are also expected to reduce conductive capacity, a trade-off

between P50 and K_s has long been hypothesized (often referred to as the hydraulic safety-

efficiency trade-off) (Tyree & Zimmermann 2002). According to this hypothesis, evolutionary

60 processes associated with frequent drought occurrence would have driven an increase of xylem

61 resistance to embolism, allowing taxa to bear lower water potentials and maintain water transport

62 at the expense of xylem conductive capacity. In contrast, increased xylem conductivity could have

63 evolved in wetter and warmer environments, where higher water transport was adaptive and

64 selective pressures favouring expensive safety features were weaker (Maherali *et al.* 2004).

65 Although this trade-off has been shown to be relatively weak across species (e.g. Maherali *et al.*

66 2004; Gleason *et al.* 2016), it remains unknown whether it reflects independent responses of each

67 trait to similar selective pressures related to climate conditions and soil properties, or a deeper

68 evolutionary integration.

69 The role of hydraulic conductivity is more nuanced when considered at the whole plant level,

70 where transport capacity needs to match water demand, which is in turn strongly influenced by

71 leaf area (Mencuccini *et al.* 2019b). Consequently, xylem conductive capacity is frequently

72 expressed in a relativized manner as a measure of hydraulic sufficiency (leaf-specific hydraulic

73 conductivity; K_l, $K_l = K_s * Hv$, see below) (Tyree & Zimmermann 2002). From this perspective,

74 plants may adapt to drought stress prioritizing supply over demand by reducing the ratio of leaf

75 area relative to cross-sectional sapwood area (i.e., increasing its inverse, the Huber value; Hv) and

76 thus ensuring the maintenance of hydraulic sufficiency under water scarcity. Contrarily, lineages

77 not exposed to drought stress and with no restriction to evolve towards a more conductive xylem

78 may be able to supply water to a higher leaf area by using a relatively low sapwood area, potentially

79 allowing for higher productivity (Mencuccini *et al.* 2019b). Therefore, we would also expect

80 xylem conductivity and sapwood-to-leaf allocation to be integrated over evolutionary timescales,

81 evolving in a coordinated manner to maintain hydraulic sufficiency (Reich *et al.* 2003).

82　In this study, we aim to elucidate the global macro-evolutionary patterns of hydraulic traits,

83　disentangling (1) the degree to which trait values are evolutionarily conserved along the

84　phylogeny, (2) the extent to which trait conservatism is related to environmentally driven selection

85　and (3) whether traits evolve in a correlated manner because of their independent responses to

86　similar environmental conditions or because of a deeper integration, in which case they may

87　represent evolutionary modules (i.e., a set of traits that co-evolve). We hypothesize that closely

88　related species will have more similar trait values than expected by chance (Losos 2008) and that

89　phylogenetic conservatism will be partly explained by environmental selection (Fig. 1). In

90　addition, we hypothesize that some pairs of traits will show signs of a direct evolutionary

91　relationship (evolutionary modules) reflecting a deep functional, developmental or genetic

92　integration. Specifically, we expect to find three evolutionary modules consistent with previously

93　hypothesized trait coordinations (namely, P50/ψ_{min}, P50/K_s, K_s/Hv).

94　**Materials and methods**

95　*Data sources*

96　We extracted detailed hydraulic trait data from a database covering 2027 species (1888

97　angiosperms and 139 gymnosperms), representing 817 genera from 161 families. Most of the data

98　come from a previously published database (Mencuccini *et al.* 2019b), which was supplemented

99　with the database reported by Liu *et al*. (2019). Species names were matched against accepted

100　names in The Plant List using the "taxonstand" R package (Cayuela *et al.* 2012). Then, the

101　"taxonlookup" R package (Pennell *et al.* 2016) was used to complete species information at the

102　genus, family, order and major evolutionary affiliation (angiosperms vs. gymnosperms) levels.

103　The database covers all major biomes (Fig. S1 in Supporting Information).

104　We used data of four hydraulic traits that were represented across sufficiently large numbers of

105 species (N > 550): (1) maximum stem-specific hydraulic conductivity (K_s, kg m^{-1} MPa^{-1} s^{-1}) as a

106 measure of xylem conductive capacity; (2) stem water potential at 50% loss of hydraulic

107 conductivity measured in terminal branches (P50, MPa) as a measure of xylem resistance to

108 embolism; (3) branch-based Huber value (Hv; cm^2 m^{-2}), defined as the sapwood cross-sectional

109 area to leaf area ratio, as a measure of allocation; and (4) minimum midday leaf water potential

110 recorded for species (ψ_{min}, MPa) as a measure of exposure to drought stress at the tissue level. We

111 also included two additional variables integrating two pairs of the four selected traits, specifically,

112 (5) maximum leaf-specific hydraulic conductivity (K_l, kg m^{-1} MPa^{-1} s^{-1}) as the hydraulic capacity

113 per unit leaf area (K_s * Hv) and (6) the hydraulic safety margin (HSM, HSM = ψ_{min} − P50) (Table

114 S1). When multiple measures for one species were available, mean values were used for all traits,

115 except for ψ_{min}, where the absolute minimum was used (c.f. Choat *et al.* 2012). For all variables,

116 we excluded data from seedlings and studies in greenhouses or experimental gardens, data

117 obtained on roots and leaves (Liu *et al.* 2019; Mencuccini *et al.* 2019b) and P50 values

118 corresponding to extreme, r-shaped vulnerability curves, following the same criteria as in Choat

119 *et al.* (2012).

120 We note that all study traits are subject to methodological uncertainty in their determination and

121 in aggregation to species level, and sample sizes differ among species. Estimates of species-

122 specific ψ_{min} in particular are sample-size dependent and likely biased to an unknown extent for

123 some species. It is likely that the sampling period will miss droughts with a long return interval at

124 some sites. It is also likely that long-lived species (e.g. several gymnosperms) will encounter more

125 severe drought events throughout their lives with consequently greater biases. HSM combines

126 uncertainties in both P50 and ψ_{min} determination, which is problematic because of direct

127 methodological issues in the case of P50 (Jansen *et al.* 2015) and because of the inherent difficulty

128   in characterizing extreme values in the case of ψ_{min} (Head *et al.* 2012). Finally, in the case of K_s,

129   although it is normalized by sapwood area, it might still depend upon stem size to some degree.

130   Sixteen environmental variables were compiled (11 related to climate and five to soil properties)

131   (Table S1). Climatic variables were extracted from WorldClim (Fick & Hijmans 2017)

132   (www.worldclim.org; accessed on February 2019) except for Moisture Index, which was extracted

133   from the global aridity and potential evapotranspiration (PET) database (Trabucco & Zomer 2019)

134   (http://www.cgiar-csi.org, data accessed on February 2019) at a resolution of 30 arcsec. Soil data

135   were extracted from SoilGrids (Hengl *et al.* 2017) (https://soilgrids.org/, accessed on February

136   2019) at the same resolution. Occurrences for all species were obtained from the Global

137   Biodiversity Information Facility (https://www.gbif.org/es/ accessed on February 2019) and the

138   Atlas of Living Australia (http://www.ala.org.au. accessed on February 2019) using the "rgbif"

139   (Chamberlain *et al.* 2020) and the "ALA4R" (Raymond, Vanderwal & Belbin 2014) R packages,

140   respectively. Potentially incorrect species occurrence records where filtered using the

141   "CoordinateCleaner" R package (Zizka *et al.* 2019).

142   *Phylogeny*

143   We used a genus-level phylogeny instead of a species-level one to avoid issues with species

144   misidentifications, which are particularly common in the tropics (Baker *et al.* 2017), and from

145   where a considerable amount of our hydraulics data come. The genera in the phylogeny covered a

146   greater number of species present in our database than the best-sampled species-level phylogeny

147   available (Smith & Brown 2018). Some models, however, were also fitted using the species-level

148   phylogeny from Smith & Brown (2018), to assess the robustness of our results to the taxonomic

149   resolution of our phylogenetic data. To construct the genus-level phylogeny, sequences of the *rbc*L

150   and *mat*K plastid gene for 707 angiosperm tree genera were obtained from Genbank

151 (www.ncbi.nlm.nih.gov/genbank/) building on previous efforts (Dexter & Chave 2016; Neves *et*

152 *al.* 2020; Segovia et al. 2020). Sequences were aligned using the MAFFT software (Katoh &

153 Standley 2013). "Ragged ends" of sequences that were missing data for most genera were

154 manually deleted from the alignment. The two chloroplast markers were concatenated, and a

155 maximum likelihood phylogeny for the genera was estimated in the RAxML v8.0.0 software

156 (Stamatakis *et al.* 2008), on the CIPRES web server (www.phylo.org), using General Time

157 Reversible (GTR) + categorical Gamma (G) model of sequence evolution. The tree was

158 constrained following order-level relationships proposed by the angiosperm Phylogeny Group IV

159 (Chase *et al.* 2016). Sequences of *Nymphaea alba* (Nymphaeaceae) were included as an outgroup.

160 The resulting maximum likelihood phylogeny for angiosperms was temporally calibrated using

161 the software treePL (Smith & O'Meara 2012). Age constraints for internal nodes were

162 implemented for most families and orders (Magallón *et al.* 2015). The rate smoothing parameter

163 (lambda) was set to 10 based on a cross-validation procedure. Finally, the newly-derived

164 angiosperm phylogeny was fused with an existing gymnosperm phylogeny (Leslie *et al.* 2018).

165 We manually added the genera *Gnetum* and *Ginkgo* according to ages found in the literature, 174

166 Ma for the Gnetales (Ran *et al.* 2018) and 265.2 Ma for Ginkgoaceae (Tank *et al.* 2015).

167 *Statistical analyses*

168 All analyses were carried out in R (3.6.0) (R Core team 2019). Some variables were transformed

169 to achieve normality (using absolute values in the case of P50 and ψ_{min}) (Table S1). A Principal

170 Components Analysis (PCA) on the 16 variables was performed using the R package "stats" (R

171 Core team 2019) to reduce the number of axes summarizing environmental variation. The first

172 principal component (PC1) explained 51% of the variance in the environmental data, representing

173 variation in water availability and some related variables such as soil pH, soil clay content, soil

174 water content and temperature seasonality, with high values characterizing more humid locations

175 with leached acidic soils characteristic of non-seasonal wet tropical habitats. The second principal

176 component (PC2) explained 20% of the variance, representing variation in energy input, with high

177 values characterizing low solar irradiation, low maximum temperatures and low atmospheric water

178 demand. Finally, the third principal component accounted for 9% of the variance and largely

179 reflected soil depth and, to a lower extent, wind velocity, with high values indicating deeper soils

180 with low sand content and low maximum wind velocities (Table S2, Fig. S2 and Fig. S3). The

181 remaining components explained a low proportion of variance (<7%), so the first three axes were

182 used to characterize the environmental niches of species in the following analyses.

183 Uni-response and bi-response Bayesian phylogenetic mixed models, alternatively including or

184 excluding fixed effects of environmental principal components, major evolutionary affiliation

185 (angiosperm vs. gymnosperm) and their interactions were fitted using the "MCMCglmm" R

186 package (Hadfield 2010) (see Table S3 for models description). All models accounted for the

187 occurrence of multiple measurements in each genus by the inclusion of genus identity as a random

188 effect. Moreover, genus-level phylogenetic relationships were taken into account as a second

189 random effect using the previously presented phylogeny. The inclusion of these random effects

190 allowed us to partition the residual variance from models into three components: the inter-generic

191 variance caused by phylogenetic relationships; the non-phylogenetic, inter-generic variance; and

192 the intra-generic variance. The inter-generic phylogenetic variance quantifies the variability

193 explained by the relationships among taxa as given by our phylogenetic hypothesis and, when

194 divided by the total variance, gives a measure of the phylogenetic signal (λ) (Lynch 1991). Non-

195 phylogenetic inter-generic variance (γ) accounts for the proportion of among-genus variability not

196 explained by the phylogeny, and the intra-generic variance (ρ) provides a measure of the

197 proportion of variability caused by intra-generic trait variation (plus any residual error) (Hadfield

198 & Nakagawa 2010) (see Appendix S1 for a more formal description).

199 To partition variances of phylogenetic and non-phylogenetic components, we implemented uni-

200 response models without fixed effects for the six selected hydraulic traits and for the three

201 environmental PCA axes as response variables (Table 1, Table S4 to see non-phylogenetic model

202 variance partitions). To identify relationships between hydraulic traits and environmental PCA

203 axes, we then ran uni-response models with hydraulic traits as response variables and single

204 environmental principal components as fixed effects, both accounting and not accounting for

205 phylogenetic relationships affecting the response trait. To examine the effect of the major split

206 between angiosperms and gymnosperms, additional models included a binary variable describing

207 major evolutionary affiliation and the interaction between affiliation and environment, allowing

208 us to detect statistical differences between angiosperms and gymnosperms in the overall mean

209 values of traits and in their relationships with environmental axes. For each group of nested

210 models, the best fitting one in terms of DIC (Deviance Information Criterion) was selected (Table

211 S5 to see DIC values). Models within 4 DIC units of each other were considered equivalent in

212 terms of fit, and the simplest one was selected.

213 Subsequently, to characterize phylogenetic covariation between the hydraulic traits and between

214 each hydraulic variable and the three environmental principal components, bi-response models

215 were used. In these models, two response variables and their phylogenetic structure were

216 considered simultaneously, resulting in a variance-covariance matrix from which the evolutionary

217 correlation between the two variables could be calculated (Appendix S1). Evolutionary

218 correlations were calculated for all combinations of trait pairs, including and excluding the three

219 environmental components, evolutionary affiliation and their interactions as fixed effects (Fig. S1

12

220   shows data coverage for each combination of traits). Finally, we also estimated evolutionary

221   correlations between traits and single environmental principal components including and

222   excluding evolutionary affiliation as a fixed effect (Table S6 to see all correlations). Bi-response

223   models were also implemented using the species-level phylogeny reported by Smith & Brown

224   (2018) and available in the R package "v.PhyloMaker" (Jin & Qian 2019), to ensure consistency

225   with genus-level results (see Apendix S2). As data availability for the species-level phylogeny was

226   lower, we replicated the bi-response genus-level models using the same reduced dataset to ensure

227   that potential differences between results were not due to different species coverage. We also

228   performed analyses using the species-level phylogeny pruned at the genus-level, to ensure that

229   potential differences between results were not explained by differences in the topologies of our

230   custom-made genus-level phylogeny and the available species-level phylogeny (Appendix S3).

231   Models were specified to achieve convergence while minimizing correlation between iterations

232   (Appendix S1). Marginal variance explained (R^2_m, variance explained by the fixed effects) and

233   conditional variance explained (R^2_c, variance explained by both fixed and random effects) were

234   calculated for the uni-response models (Nakagawa & Schielzeth 2013). P-values were calculated

235   for evolutionary correlations following Makowski *et al*. (2019).

236   Finally, reconstructions of the six traits and the three environmental principal components

237   evolution under a Brownian motion model were mapped along the phylogeny using maximum

238   likelihood ancestral state reconstructions (Schluter *et al*. 1997) by means of the "Phytools" R

239   package (Revell 2013).

Results

Phylogenetic and non-phylogenetic variances

All six selected traits showed a significant phylogenetic signal. The proportion of variance that was explained by the inter-generic phylogenetic structure (λ) ranged from 0.432 (K_l) to 0.745 (ψ_{min}) (Table 1). This means that 43.2-74.5% of trait variances can be attributed to relatively deep evolutionary differences among genera, with the rest being attributed to non-phylogenetically correlated inter-generic (γ) and intra-generic (ρ) variances. Intra-generic variances (ρ) ranged from 0.189 (ψ_{min}) to 0.532 (K_l), being the second most important variance component in all cases except K_l (where it was the most important), indicating that trait diversification within genera is a substantial generator of global trait variability. Analyses using the species-level phylogeny confirmed that variation within genera also had strong phylogenetic patterns (Appendix S2). Finally, inter-generic, non-phylogenetically related variances (γ) ranged from 0.036 (K_l) to 0.225 (P50) and accounted for the lowest proportion of the variance in all cases (Table 1). Phylogenetic mapping of hydraulic traits qualitatively confirmed the findings reported above, showing more gradual changes in highly conserved traits such as ψ_{min} and changes more concentrated at the tips of the phylogeny for variables showing a lower phylogenetic signal, such as Hv, which also showed higher intra-generic variance (Fig. 2, Fig. 3 and Fig. S4).

Importantly, the phylogenetic signal of the three environmental principal components was also very high, particularly for PC1, representing water availability (0.820) and PC3, mainly represented by soil depth (0.841) (Table 1, Fig. S5).

Environmental drivers of hydraulic trait variability

In models that accounted for phylogenetic structure, all hydraulic traits showed significant relationships with at least one of the three environmental axes defined by the PCA (Fig. 4).

14

263   Conditional explained variances (R^2_c) were notably higher than marginal explained variances

264   (R^2_m), indicating that accounting for the phylogenetic relationships was crucial to improve model

265   fit (Fig. 4). Consistent with the fact that environmental axes were highly phylogenetically

266   conserved, we also found that the phylogenetic signal of traits (Table 1) diminished when

267   accounting for environmental effects (Fig. 4, lambdas (λ)), thus indicating that environmental

268   conditions explain part of the phylogenetic variance.

269   Xylem resistance to embolism (|P50|) was only negatively related to PC1 (water availability).

270   Minimum water potential at midday ($|\psi_{min}|$) was negatively related to PC1 and PC2 (declining

271   energy input) and positively to PC3 (soil depth). However, the relationship with PC1 was only

272   significant for angiosperms. Xylem conductivity (K_s) was found to be positively related to PC1

273   and PC3, being negatively related with PC2 only in non-phylogenetic models. Sapwood to leaf

274   area ratio (Hv) was negatively related to PC1 and PC3. The hydraulic safety margin (HSM) was

275   positively related to PC1 and PC2 only for angiosperms and the relationship between HSM and

276   PC3 was only significant (and negative) for non-phylogenetic models. Finally, Leaf-specific

277   conductivity (K_l) was only related to PC2 (negatively) in phylogenetic models, but a positive

278   relationship with PC3 was also found when using non-phylogenetic models (Fig. 4).

279   *Evolutionary correlations*

280   Significant evolutionary correlations were reported between $|\psi_{min}|$ and |P50| (positive), K_s and Hv

281   (negative), Hv and |P50| (positive) (Fig. 5). These evolutionary correlations were confirmed when

282   the species-level phylogeny was used, which also showed a significant evolutionary correlations

283   between |P50| and K_s (negative), $|\psi_{min}|$ and Hv (positive) and K_s and $|\psi_{min}|$ (negative) (Fig. S6). The

284   emergence of these evolutionary correlations was not explained by the lower number of species

285   available for the species-level phylogeny compared to the genus-level one, nor by differences in

286   topology between phylogenies (Appendix S3), so it is likely due to the large amount of

287   phylogenetic covariance between traits within genera. Only two evolutionary correlations between

288   traits remained once environmental factors and major evolutionary affiliation of species were

289   accounted for, coinciding with two of the three hypothesized evolutionary modules. These were

290   the ones involving |P50| and $|\psi_{min}|$ (positive correlation) and K_s and Hv (negative correlation) (Fig.

291   5, Fig. S6). While |P50| and $|\psi_{min}|$ presented a highly conserved covariation pattern, the

292   evolutionary integration between K_s and Hv was less strong. The latter was marginally significant

293   when using the genus-level phylogeny (Fig. 5), but clearly significant when intra-generic

294   phylogenetic covariation between traits was additionally considered by using the species-level

295   phylogeny (Fig, S6).

296   Consistent evolutionary correlations were also observed between certain hydraulic traits and

297   environmental principal components in the bi-response models: K_s was positively correlated with

298   PC1 (water availability), and PC3 (soil depth) while its relationship with PC2 (energy input) was

299   only significant at the genus-level and disappeared when considering major evolutionary

300   affiliation. Hv was negatively correlated with PC1 and PC3; and both |P50| and $|\psi_{min}|$ were

301   negatively correlated with PC1 (Fig. 5).

302   **Discussion**

303   *Conservatism and adaptation in hydraulic trait evolution*

304   We found a clear pattern of phylogenetic conservatism for hydraulic traits, suggesting that the

305   legacy of traits found in species' evolutionary ancestors is an important determinant of trait values

306   in extant species. While we cannot formally rule out Brownian motion evolution operating over

307   long evolutionary timescales as the source of present-day trait variability on the basis of our single

308   trait variance partitioning (Revell *et al*. 2008), our finding of evolutionary correlations of traits

309 with environmental variables indicates a key role for non-random evolutionary processes.

310 Moreover, environmental components explained part of traits' phylogenetic variance when

311 accounted for as fixed effects (Fig. 4). Therefore, our analyses indicate that adaptive processes

312 have driven the diversification of hydraulic traits, but the prevalent pattern of phylogenetic niche

313 conservatism suggests that evolutionary constraints have limited the range of trait values within

314 lineages. Thus, lineages have been largely tracking environments similar to those their ancestors

315 were already adapted to, retaining ancestral traits because of stabilizing selection (Ackerly 2009),

316 while occasionally adapting to novel environmental conditions.

317 We do observe a wide range of trait values across lineages (including among genera), indicating

318 that they adaptively diverged in deep evolutionary time (Fig. 2, Fig. 3, Fig. S4 and Fig. S5).

319 Further, substantial trait variation can also arise over shorter evolutionary timescales (i.e., in recent

320 evolutionary time) via species adapting to present-day selective pressures, as supported by the

321 significant degree of trait variance at the intra-generic level (Table 1), which also appears to have

322 a phylogenetic component (Fig. S6, Appendix 2). As a result, lineages that have been evolving in

323 dry habitats have adapted to a higher exposure to drought stress by increasing their xylem

324 resistance to embolism, being able to maintain water transport at low water potentials (Choat *et al.*

325 2012). These species are also selected to ensure water supply to leaves by using a relatively high

326 sapwood area with a low hydraulic conductivity (Mencuccini *et al.* 2019b). As water become less

327 limiting, lineages are less exposed to low water potentials and are not selected to increase xylem

328 resistance to embolism, while switching their allocation priority to a high leaf area maintained by

329 a smaller area of highly conductive sapwood (Fig. 4).

330 However, substantial variability in species exposure to drought stress within a given environment

331 reflects the fact that plant characteristics such as stomatal control (Brodribb & McAdam 2017),

332 deciduousness (Wolfe *et al.* 2016) or rooting depth (Canadell *et al.* 1996) are also determining

333 hydraulic trait evolution. This may explain the lack of a relationship between PC1 (water

334 availability) and ψ_{min} and HSM in gymnosperms, a clade mainly represented by Pinaceae and

335 Cupressaceae (Fig. S7) that are known to adopt contrasting strategies under drought. While

336 Pinaceae avoid exposure to low water potentials by closing their stomata and possibly

337 disconnecting from the soil (Poyatos *et al.* 2018), Cupressaceae tolerate them by presenting a high

338 resistance to embolism (Brodribb *et al.* 2014). Differences between angiosperms and

339 gymnosperms could also be due to an underestimation of drought stress exposure for long-lived

340 gymnosperms, especially in the case of the highly stress-resistant Cupressaceae, for which the

341 observation window may not have been long enough to adequately capture ψ_{min}. Therefore,

342 different evolutionary processes may be dominant depending on the taxon studied. For instance,

343 xylem resistance has been reported to be extremely labile for the genus *Callitris* (Larter *et al.*

344 2017) and to be conserved for *Juniperus* (Willson *et al.* 2008), while showing a high canalization

345 for *Pinus* species (Lamy *et al.* 2014). It is also worth noting that our global eco-evolutionary

346 overview may be limited by the availability of hydraulic data and its methodological uncertainties,

347 as well as by the difficulty of upscaling traits at the whole-plant level, which remains a challenge

348 (Mencuccini *et al.* 2019a).

349 *Evolutionary modules in hydraulic traits*

350 Traits can evolve in an apparently coordinated fashion because of their response to similar selective

351 pressures, but direct relationships between them may also arise from functional, developmental or

352 genetic constraints, conforming to evolutionary modules. We found two sets of traits for which an

353 evolutionary correlation cannot be explained by similar, albeit independent responses to

354 environmental conditions or by fundamental differences between angiosperms and gymnosperms.

355 These sets of traits represent a deeper evolutionary integration, confirming two of the three

356 hypothesized evolutionary modules. The first evolutionary module involves species exposure to

357 drought and resistance to embolism (P50/ψ_{min}), and it is strongly conserved over evolutionary

358 scales. The second one involves xylem conductivity and sapwood to leaf area allocation (K_s/Hv),

359 the integration of which appears stronger when quantified in more recent evolutionary time (c.f.

360 results for genus- vs. species-level phylogenies in Fig. 5 and Fig. S6). The third evolutionary

361 module we hypothesized (K_s/P50) appears to be explained exclusively by separate trait responses

362 to similar selective pressures, confirming previous results (Maherali *et al.* 2004). Therefore, a

363 direct evolutionary trade-off between K_s and P50 can be rejected based on available data, further

364 indicating that K_s and P50 cannot be determined by a single common anatomical feature (e.g., the

365 size distribution of pores in the inter-conduit pit membranes) (Baas *et al.* 2004). We suggest that

366 K_s and P50 depend on several anatomical properties that may be coordinated under strong selective

367 pressures, but do not necessarily co-evolve when pressures are relaxed over evolutionary

368 timescales. Our results likely reflect the fact that some species may present strategies that do not

369 rely on maximizing xylem conductivity or resistance to embolism, especially when water is not

370 the most limiting resource and survival does not depend on fast resource use (Reich 2014).

371 However, the detailed structural and physiological conditions allowing the independent evolution

372 of these two traits remains to be elucidated.

373 Traits involved in the same evolutionary module are likely to be functionally, developmentally

374 and genetically integrated. Deep functional integrations over evolutionary times can be explained

375 by the need to optimize HSM and K_l under a given environmental context, as the maintenance of

376 positive safety margins and a sufficient hydraulic supply to leaves are likely to be closely linked

377 to survival (Choat *et al.* 2018) and under a strong stabilizing selection. Therefore, events of

378 coordinated directional selection on the involved trait pairs described above might take place over

379 evolutionary times in order to maintain HSM and K_l values close to the adaptive peak. The

380 conservative nature of the relationship between Hv and K_s also reflects broader strategies of

381 convergent evolution integrating hydraulic with photosynthetic and nutrient-use traits as a function

382 of water availability (Hao *et al.* 2011; Liu *et al.* 2015).

383 Integration might also be influenced by phylogenetic conservatism in underlying physiological

384 processes and anatomical features. For example, conservatism in stomatal control (Brodribb &

385 McAdam 2017) and leaf phenology (Davies *et al.* 2013) might explain the evolutionary covariation

386 between ψ_{min} and P50 beyond environmental forcing, with some lineages being able to avoid low

387 water potentials by rapid stomatal closure (Martin-StPaul *et al.* 2017) or drought-deciduousness

388 (Kolb & Davis 1994).

389 Finally, these functional and developmental integrations may be underpinned by genetic

390 integration, specifically meaning that processes such as genetic correlation (Etterson & Shaw

391 2001), linkage disequilibrium and pleiotropy (Cheverud 1996) might be affecting the anatomical

392 and structural determinants of the traits involved, leading to the observed evolutionary integration.

393 As a result, the evolution of traits in the same module might be genetically constrained (Wagner

394 1996). Further work on the causes and consequences of the evolutionary integration of hydraulic

395 traits, and the meaning of their conservatism through evolutionary time, will be crucial to

396 characterize global trait syndromes and assess species adaptive potential under changing

397 environmental conditions.

Conclusion

Hydraulic traits are under strong selective control and appear to be largely determined by deep-time evolutionary changes driven by adaptation to divergent environmental conditions, in turn limited by evolutionary constraints. We have found evidence for evolutionary integrations not explained by common environmental drivers, conforming to two evolutionary modules: the xylem resistance-exposure module (ψ_{min}/P50), which is highly conserved over evolutionary scales, and the conductivity-allocation module (Hv/K_s), which is more evident in recent evolutionary time. Our results do not support the hypothesized resistance-conductivity module (K_s/P50). The underlying mechanisms shaping these evolutionary modules and their role in species functional and evolutionary diversification remain to be elucidated. More phylogenetically explicit studies of individual clades (including intraspecific genetic, anatomical and functional variation) under different environmental contexts will allow further characterization of plant trait syndromes as a network of integrated units that respond to natural selection.

421   APOYO CCTE AFB170008. The data derived from the hydraulics database are partly an outcome

422   from a working group funded by the Australian Research Council (ARC) through the Australia-

423   New Zealand Research Network for Vegetation Function.

424   **Literature cited**

425   Ackerly, D. (2009). Conservatism and diversification of plant functional traits: Evolutionary rates

426   versus phylogenetic signal. *Proc. Natl. Acad. Sci.*, 106, 19699–19706.

427   Adams, H.D., Zeppel, M.J.B., Anderegg, W.R.L., Hartmann, H., Landhäusser, S.M., Tissue, D.T.,

428   *et al*. (2017). A multi-species synthesis of physiological mechanisms in drought-induced tree

429   mortality. *Nat. Ecol. Evol.*, 1, 1285–1291.

430   Baas, P., Ewers, F.W., Davis, S.D. & Wheeler, E.A. (2004). Evolution of xylem physiology. In:

431   (The evolution of plant physiology) {Hemsley, A.R., Poole, L.}. Elsevier, London, 273–295.

432   Baker, T. R., Pennington, R. T., Dexter, K. G., Fine, P. V. A., Fortune-Hopkins, H., Honorio, E.

433   N., *et al*. (2017). Maximising Synergy among Tropical Plant Systematists, Ecologists, and

434   Evolutionary Biologists. *Trends Ecol Evol.*, 32(4), 258–267.

435   Bhaskar, R. & Ackerly, D.D. (2006). Ecological relevance of minimum seasonal water potentials.

436   *Physiol. Plant.*, 127, 353–359.

437   Brodribb, T. & Hill, R.S. (1999). The importance of xylem constraints in the distribution of conifer

438   species. *New Phytol.*, 143, 365–372.

439   Brodribb, T.J. & McAdam, S.A.M. (2017). Evolution of the stomatal regulation of plant water

440   content. *Plant Physiol.*, 174, 639–649.

441   Brodribb, T.J., McAdam, S.A.M., Jordan, G.J. & Martins, S.C.V. (2014). Conifer species adapt to

442   low-rainfall climates by following one of two divergent pathways. *Proc. Natl. Acad. Sci.*, 111,

443   14489–14493.

444   Canadell, J., Jackson, R.B., Ehleringer, J.R., Mooney, H.A., Sala, O.E. & Schulze, E.D. (1996).

445   Maximum rooting depth of vegetation types at the global scale. *Oecologia*, 108, 583–595.

446   Cayuela, L., Granzow-de la Cerda, Í., Albuquerque, F.S. & Golicher, D.J. (2012). Taxonstand: An

447   r package for species names standardisation in vegetation databases. *Methods Ecol. Evol.*, 3, 1078–

448   1083.

449   Chamberlain S., Barve V., Mcglinn D., Oldoni D., Desmet P., Geffert L. & Ram K. (2020). rgbif:

450   Interface to the Global Biodiversity Information Facility API. R package version 2.2.0.

451   Chase, M.W., Christenhusz, M.J.M., Fay, M.F., Byng, J.W., Judd, W.S., Soltis, D.E., *et al*. (2016).

452   An update of the Angiosperm Phylogeny Group classification for the orders and families of

453   flowering plants: APG IV. *Bot. J. Linn. Soc.*, 181, 1–20.

454   Cheverud, J.M. (1996). Developmental integration and the evolution of pleiotropy. *Am. Zool.*, 36,

455   44–50.

456   Choat, B., Brodribb, T., Brodersen, C., Duursma, R., López, R. & Medlyn, B. (2018). Triggers of

457   tree mortality under drought drought and forest mortality. *Nature*, 558, 531–539.

458   Choat, B., Jansen, S., Brodribb, T.J., Cochard, H., Delzon, S., Bhaskar, R., *et al*. (2012). Global

459   convergence in the vulnerability of forests to drought. *Nature*, 491, 752–755.

460   Davies, T.J., Wolkovich, E.M., Kraft, N.J.B., Salamin, N., Allen, J.M., Ault, T.R., *et al*. (2013).

461   Phylogenetic conservatism in plant phenology. *J. Ecol.*, 101, 1520–1530.

462   Dexter, K. & Chave, J. (2016). Evolutionary patterns of range size, abundance and species richness

463   in Amazonian angiosperm trees. *PeerJ*, 2016, 1–14.

464   Dixon, H.H. (1914). *Transpiration and the ascent of sap in plants.* MacMillan, London, UK.

465   Etterson, J.R. & Shaw, R.G. (2001). Constraint to adaptive evolution in response to global

466   warming. *Science*, 294, 151–154.

467   Fick, S.E. & Hijmans, R.J. (2017). WorldClim 2: new 1-km spatial resolution climate surfaces for

468   global land areas. *Int. J. Climatol.*, 37, 4302–4315.

469   Gleason, S.M., Westoby, M., Jansen, S., Choat, B., Hacke, U.G., Pratt, R.B., *et al.* (2016). Weak

470   trad eoff between xylem safety and xylem-specific hydraulic efficiency across the world's woody

471   plant species. *New Phytol.*, 209, 123–136.

472   Hadfield, J.D. (2010). MCMCglmm for R. J. *Stat. Softw.*, 33.

473   Hadfield, J.D. & Nakagawa, S. (2010). General quantitative genetic methods for comparative

474   biology: Phylogenies, taxonomies and multi-trait models for continuous and categorical

475   characters. *J. Evol. Biol.*, 23, 494–508.

476   Hao, G.Y., Goldstein, G., Sack, L., Holbrook, N.M., Liu, Z.H., Wang, A.Y., *et al*. (2011). Ecology

477   of hemiepiphytism in fig species is based on evolutionary correlation of hydraulics and carbon

478   economy. *Ecology*, 92, 2117–2130.

479   He, P., Gleason, S.M., Wright, I.J., Weng, E., Liu, H., Zhu, S., *et al*. (2020). Growing-season

480   temperature and precipitation are independent drivers of global variation in xylem hydraulic

481   conductivity. *Glob. Chang. Biol.*, 26, 1833–1841.

482   Head, A.W., Hardin, J.S. & Adolph, S.C. (2012). Methods for estimating peak physiological

483   performance and correlating performance measures. *Environ. Ecol. Stat.*, 19, 127–137.

484   Hengl, T., Mendes de Jesus, J., Heuvelink, G. B. M., Ruiperez Gonzalez, M., Kilibarda, M.,

485   Blagotić, A., *et al*. (2017). SoilGrids250m: Global gridded soil information based on machine

486   learning. *PloS One*, 12(2), e0169748.

487   Jansen, S., Schuldt, B. & Choat, B. (2015). Current controversies and challenges in applying plant

488   hydraulic techniques. *New Phytol.*, 205, 961–964.

489   Jin, Y. & Qian, H. (2019). V.PhyloMaker: an R package that can generate very large phylogenies

490   for vascular plants. *Ecography*, 42, 1353–1359.

491   Katoh, K. & Standley, D.M. (2013). MAFFT multiple sequence alignment software version 7:

492   Improvements in performance and usability. *Mol. Biol. Evol.*, 30, 772–780.

493   Kolb, K.J. & Davis, S.D. (1994). Drought Tolerance and Xylem Embolism in Co-Occurring

494   Species of Coastal Sage and Chaparral. *Ecology*, 75, 648–659.

495   Lamy, J.B., Delzon, S., Bouche, P.S., Alia, R., Vendramin, G.G., Cochard, H., *et al.* (2014).

496   Limited genetic variability and phenotypic plasticity detected for cavitation resistance in a

497   Mediterranean pine. *New Phytol.*, 201, 874–886.

498   Larter, M., Pfautsch, S., Domec, J.C., Trueba, S., Nagalingum, N. & Delzon, S. (2017). Aridity

499   drove the evolution of extreme embolism resistance and the radiation of conifer genus Callitris.

500   *New Phytol.*, 215, 97–112.

501 Leslie, A.B., Beaulieu, J., Holman, G., Campbell, C.S., Mei, W., Raubeson, L.R., *et al*. (2018). An

502 overview of extant conifer evolution from the perspective of the fossil record. *Am. J. Bot.*, 105,

503 1531–1544.

504 Liu, H., Gleason, S.M., Hao, G., Hua, L., He, P., Goldstein, G., *et al.* (2019). Hydraulic traits are

505 coordinated with maximum plant height at the global scale. *Sci. Adv.*, 5, eaav1332.

506 Liu, H., Xu, Q., He, P., Santiago, L.S., Yang, K. & Ye, Q. (2015). Strong phylogenetic signals and

507 phylogenetic niche conservatism in ecophysiological traits across divergent lineages of

508 Magnoliaceae. *Sci. Rep.*, 5, 1–12.

509 Losos, J.B. (2008). Phylogenetic niche conservatism, phylogenetic signal and the relationship

510 between phylogenetic relatedness and ecological similarity among species. *Ecol. Lett.*, 11, 995–

511 1003.

512 Lynch, M. (1991). Methods for the analysis of comparative data in evolutionary biology.

513 *Evolution*, 45, 1065–1079.

514 Magallón, S., Gómez-Acevedo, S., Sánchez-Reyes, L.L. & Hernández-Hernández, T. (2015). A

515 metacalibrated time-tree documents the early rise of flowering plant phylogenetic diversity. *New

516 Phytol.*, 207, 437–453.

517 Maherali, H., Pockman, W.T. & Jackson, R.B. (2004). Adaptive variation in the vulnerability of

518 woody plants to xylem cavitation. *Ecology*, 85, 2184–2199.

519 Makowski, D., Ben-Shachar, M. & Lüdecke, D. (2019). bayestestR: Describing Effects and their

520 Uncertainty, Existence and Significance within the Bayesian Framework. J. *Open Source Softw.*,

521 4, 1541.

522 Martin-StPaul, N., Delzon, S. & Cochard, H. (2017). Plant resistance to drought depends on timely

523 stomatal closure. *Ecol. Lett.*, 20, 1437–1447.

524 Mencuccini, M., Manzoni, S. & Christoffersen, B. (2019a). Modelling water fluxes in plants: from

525 tissues to biosphere. *New Phytol.*, 222, 1207-1222.

526 Mencuccini, M., Rosas, T., Rowland, L., Choat, B., Cornelissen, H., Jansen, S., *et al*. (2019b).

527 Leaf economics and plant hydraulics drive leaf : wood area ratios. *New Phytol.* 224, 1544-1556.

528 Nakagawa, S. & Schielzeth, H. (2013). A general and simple method for obtaining R2 from

529 generalized linear mixed-effects models. *Methods Ecol. Evol.*, 4, 133–142.

530 Neves, D.M., Dexter, K.G., Baker, T.R., Coelho de Souza, F., Oliveira-Filho, A.T., Queiroz, L.P.,

531 *et al*. (2020). Evolutionary diversity in tropical tree communities peaks at intermediate

532 precipitation. *Sci. Rep.*, 10, 1188.

533 Pennell, M.W., FitzJohn, R.G. & Cornwell, W.K. (2016). A simple approach for maximizing the

534 overlap of phylogenetic and comparative data. *Methods Ecol. Evol.*, 7, 751–758.

535 Poyatos, R., Aguadé, D. & Martínez-Vilalta, J. (2018). Below-ground hydraulic constraints during

536 drought-induced decline in Scots pine. *Ann. For. Sci.*, 75.

537 Ran, J.H., Shen, T.T., Wang, M.M. & Wang, X.Q. (2018). Phylogenomics resolves the deep

538 phylogeny of seed plants and indicates partial convergent or homoplastic evolution between

539 Gnetales and angiosperms. *Proc. R. Soc. B Biol. Sci.*, 285.

540 Raymond, B., Vanderwal, J., & Belbin, L., (2014). ALA4R version 1.01. Atlas of Living

541 Australia.

542   R Core Team (2017). R: A language and environment for statistical computing. R Foundation for

543   Statistical Computing, Vienna, Austria.

544   Reich, P. B., Wright, I. J., Cavender-Bares, J., Craine, J. M., Oleksyn, J., Westoby, M., *et al*.

545   (2003). The Evolution of Plant Functional Variation: Traits, Spectra, and Strategies. *Int. J. Plant*

546   *Sci.*, 164(S3), S143–S164.

547   Reich, P.B. (2014). The world-wide "fast-slow" plant economics spectrum: A traits manifesto. *J.*

548   *Ecol.*, 102, 275–301.

549   Revell, L.J. (2013). Two new graphical methods for mapping trait evolution on phylogenies.

550   *Methods Ecol. Evol.*, 4, 754–759.

551   Revell, L.J., Harmon, L.J. & Collar, D.C. (2008). Phylogenetic signal, evolutionary process, and

552   rate. *Syst. Biol.*, 57, 591–601.

553   Schluter, D., Price, T., Mooers, A. Ø., & Ludwig, D. (1997). Likelihood of ancestor states in

554   adaptive radiation. *Evolution*, 51(6), 1699–1711.

555   Segovia, R.A., Pennington, R.T., Baker, T.R., De Souza, F.C., Neves, D.M., Davis, C.C., *et al*.

556   (2020). Freezing and water availability structure the evolutionary diversity of trees across the

557   Americas. *Sci. Adv.*, 6(19), eaaz5373.

558   Smith, S.A. & Brown, J.W. (2018). Constructing a broadly inclusive seed plant phylogeny. *Am. J.*

559   *Bot.*, 105, 302–314.

560   Smith, S.A. & O'Meara, B.C. (2012). TreePL: Divergence time estimation using penalized

561   likelihood for large phylogenies. *Bioinformatics*, 28, 2689–2690.

562 Sperry, J.S. & Hacke, U.G. (2002). Desert shrub water relations with respect to soil characteristics

563 and plant functional type. *Funct. Ecol.*, 16, 367–378.

564 Stamatakis, A., Hoover, P. & Rougemont, J. (2008). A rapid bootstrap algorithm for the RAxML

565 web servers. *Syst. Biol.*, 57, 758–771.

566 Tank, D.C., Eastman, J.M., Pennell, M.W., Soltis, P.S., Soltis, D.E., Hinchliff, C.E., *et al*. (2015).

567 Nested radiations and the pulse of angiosperm diversification: increased diversification rates often

568 follow whole genome duplications. *New Phytol.*, 207, 454–467.

569 Trabucco, A. & Zomer, R.. (2019). Global Aridity Index and Potential Evapotranspiration (ET0)

570 Climate Database v2.

571 Tyree M.T. & Zimmermann M.H. (2002). *Xylem Structure and the Ascent of Sap.* Springer, New

572 York.

573 Venturas, M.D., Sperry, J.S. & Hacke, U.G. (2017). Plant xylem hydraulics: What we understand,

574 current research, and future challenges. *J. Integr. Plant Biol.*, 59, 356–389.

575 Wagner, G.P. (1996). Homologues, natural kinds and the evolution of modularity. *Am. Zool.*, 36,

576 36–43.

577 Willson, C.J., Manos, P.S. & Jackson, R.B. (2008). Hydraulic traits are influenced by phylogenetic

578 history in the drought-resistant, invasive genus *Juniperus* (Cupressaceae). *Am. J. Bot.*, 95, 299–

579 314.

580 Wolfe, B.T., Sperry, J.S. & Kursar, T.A. (2016). Does leaf shedding protect stems from cavitation

581 during seasonal droughts? A test of the hydraulic fuse hypothesis. *New Phytol.*, 212, 1007–1018.

582 Zanne, A.E., Tank, D.C., Cornwell, W.K., Eastman, J.M., Smith, S.A., Fitzjohn, R.G., *et al*.

583 (2014). Three keys to the radiation of angiosperms into freezing environments. *Nature*, 506, 89–

584 92.

585 Zizka, A., Silvestro, D., Andermann, T., Azevedo, J., Duarte Ritter, C., Edler, D., *et al*. (2019).

586 CoordinateCleaner: Standardized cleaning of occurrence records from biological collection

587 databases. *Methods Ecol. Evol.*, 10, 744–751.

Tables

Table 1. Variance partitioning for six hydraulic traits and three environmental principal components related to water availability (PC1), energy input (PC2) and soil depth (PC3). Legend: N: number of species used in each case (for which both phylogenetic and hydraulic data were available), phylogenetic variance (phylogenetic signal, λ), non-phylogenetic inter-generic variance (γ) and intra-generic variance plus measurement error (ρ). Mean and lower and upper 95% credible intervals (HDP) are shown for each component.

variable	N	λ	Lower HPD	Upper HPD	γ	Lower HDP	Upper HDP	ρ	Lower HDP	Upper HDP
Log(|P50|)	868	0.484	0.305	0.697	0.225	0.085	0.360	0.291	0.205	0.368
Log(|ψ_{min}|)	541	0.745	0.572	0.874	0.066	0.000	0.179	0.189	0.129	0.273
log(K_s)	1026	0.515	0.363	0.680	0.086	0.000	0.174	0.399	0.303	0.493
Log(Hv)	1271	0.446	0.291	0.594	0.191	0.097	0.294	0.363	0.276	0.449
HSM	326	0.449	0.201	0.722	0.163	0.000	0.339	0.388	0.246	0.546
Log(K_l)	827	0.432	0.244	0.592	0.036	0.000	0.113	0.532	0.399	0.675
PC1	1911	0.820	0.767	0.870	0.063	0.030	0.099	0.117	0.093	0.139
PC2	1911	0.686	0.599	0.766	0.028	0.000	0.069	0.286	0.230	0.341
PC3	1911	0.841	0.798	0.876	0.007	0.000	0.027	0.152	0.124	0.182

595

596 **Figure captions**

597 **Figure 1.** Hypotheses and theoretical framework. Double-headed arrows represent potential

598 evolutionary correlation involving key hydraulic traits (xylem conductivity (K_s), xylem resistance

599 to embolism (P50), sapwood allocation relative to leaf area (Huber value, Hv) and drought

600 exposure (ψ_{min})). HSM refer to Hydraulic Safety Margin, which is the relationship between ψ_{min}

601 and P50, and K_l refer to the hydraulic sufficiency, which is the relationship between K_s and Hv.

602 Lines represent evolutionary relationships tested between pairs of traits. Blue lines represent

603 hypothetical positive relationships between traits, and red lines hypothetical negative ones. Black

604 curved arrows represent traits phylogenetic variance (phylogenetic signal). Each hypothesized

605 coordination between traits is also encircled using long dashed lines and labelled accordingly.

606 **Figure 2.** Phylogenetic reconstruction of drought exposure (ψ_{min}) and embolism resistance (P50)

607 under a Brownian motion model of evolution. Reconstructions are made log-transformed absolute

608 values in both cases. Families with more than one genus are presented and some of the most

609 important families are highlighted in bold. Gymnosperm families are displayed in grey and

610 angiosperm families in black.

611 **Figure 3.** Phylogenetic reconstruction of hydraulic conductivity (K_s) and sapwood allocation

612 relative to leaf area (Huber value, Hv). Reconstructions are made on log-transformed data in both

613 cases. Families with more than one genus are presented and some of the most important families

614 are highlighted in bold. Gymnosperm families are displayed in grey and angiosperm families in

615 black.

616 **Figure 4.** Trait-environment relationships. Relationships between environmental principal

617 components (PC1, which is related to water availability; PC2, which is related to energy input and

32

618 PC3, which is mainly related to soil depth) and hydraulic traits (log-transformed absolute values)

619 accounting for the phylogenetic structure of the hydraulic traits. The best model for each case is

620 displayed, showing the Spermatophyte level relationship (black) or the angiosperm and

621 gymnosperm relationships (red and blue, respectively) when statistically different. Grey dashed

622 lines represent the regression line at the Spermatophyte level without accounting for the

623 phylogenetic structure. Statistically significant ($p < 0.05$) regression slopes are displayed in bold

624 following the same colour code. Signif. codes: '***': $P < 0.001$; '**': $P < 0.01$; '*': $P < 0.05$ '.':

625 $P < 0.1$ ' ': $P > 0.1$. Residual phylogenetic signal (λ) once environmental effects are accounted for

626 in each case is reported when relationships are significant. R^2_m is the variance explained by the

627 fixed effects and R^2_c by the fixed and random effects for the phylogenetic mixed models.

628 **Figure 5.** Evolutionary correlations between hydraulic traits and between traits and environmental

629 principal components (PC1, which is related to water availability; PC2, which is related to energy

630 input and PC3, which is mainly related to soil depth). Environmental variables represent

631 orthogonal PC axes and as such are not correlated. Lines represent significant evolutionary

632 correlations (i.e., when the credible interval for the estimated correlation does not include zero),

633 with the thickness of the line proportional to the strength of the correlation coefficient (also given

634 on the same line). Light red lines represent negative relationships, dark blue lines indicate positive

635 relationships. Significant correlation coefficients between traits when excluding environmental

636 components and evolutionary affiliation as fixed effects are shown in italics, and significant

637 correlation coefficients between traits including environmental components and evolutionary

638 affiliation as fixed effects are shown in bold (in the case of the relationships between

639 environmental axes and traits, only evolutionary affiliation was considered). Dashed lines

640 represent evolutionary correlations that became non-significant when environmental effects and

33

641   major evolutionary affiliations were considered. Pie charts represent phylogenetic signal (dark),

642   inter-generic (medium) and intra-generic (light) variances reported in Table 1, calculated using the

643   maximum number of observations for each case. P-values are also displayed for each coefficient.

644   Signif. codes: '***': $P < 0.001$; '**': $P < 0.01$; '*': $P < 0.05$ '.': $P < 0.1$ ' ': $P > 0.1$.

645   **Figure 1**

646

647　**Figure 2**
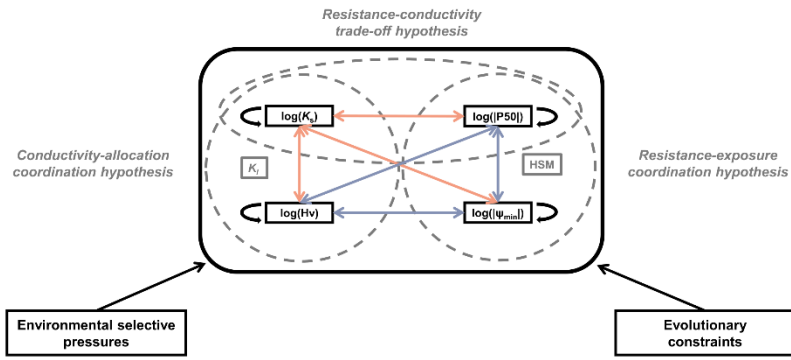
Drought exposure (log($|\psi_{min}|$))

Embolism resistance (log($|P50|$))

648

36
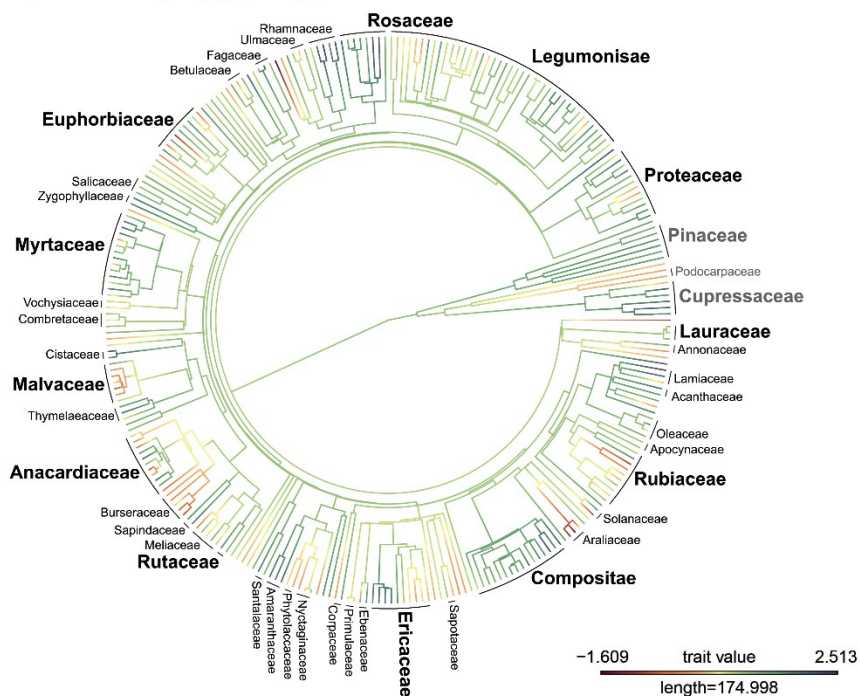
Conductivity (log(K_s))
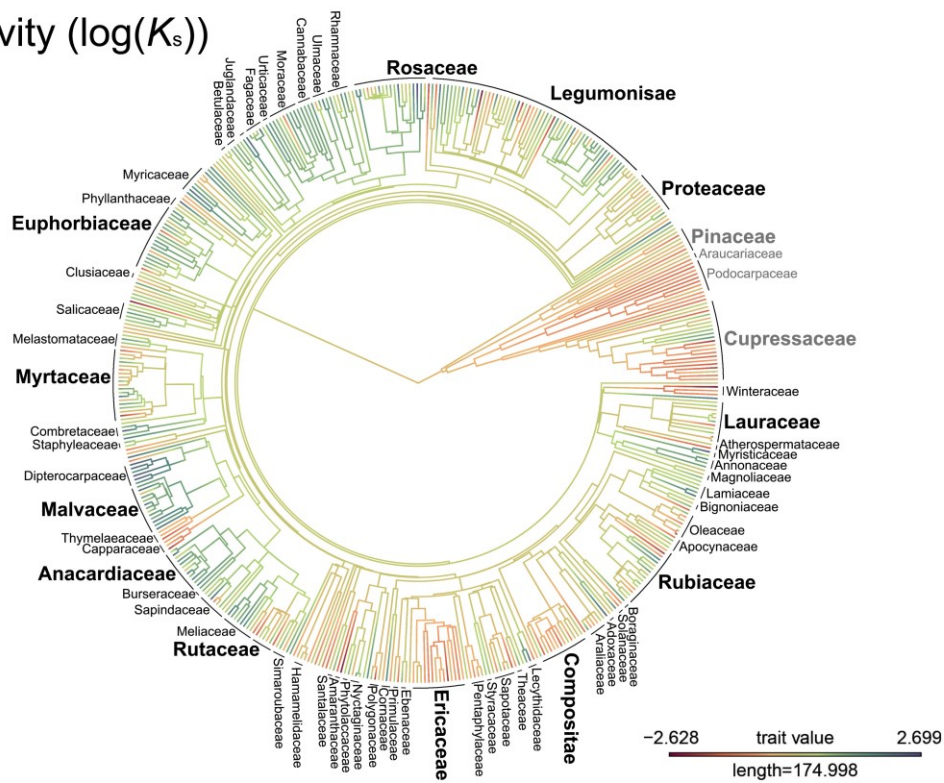
Sapwood/leaf allocation (log(Hv))

Figure 4

652 **Figure 5**

653
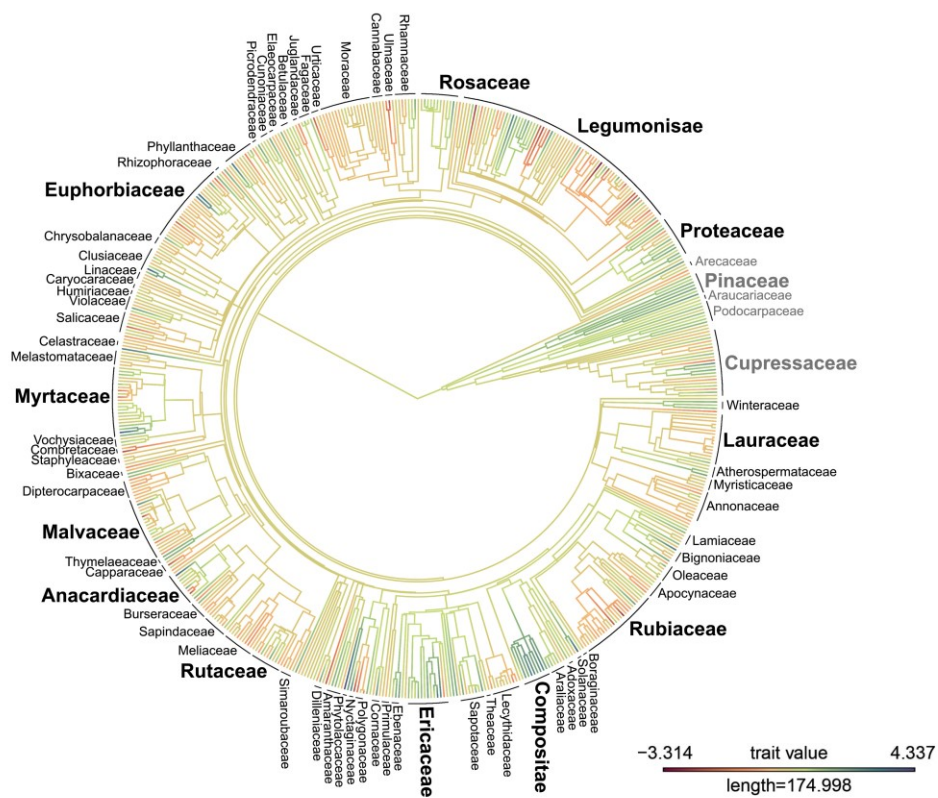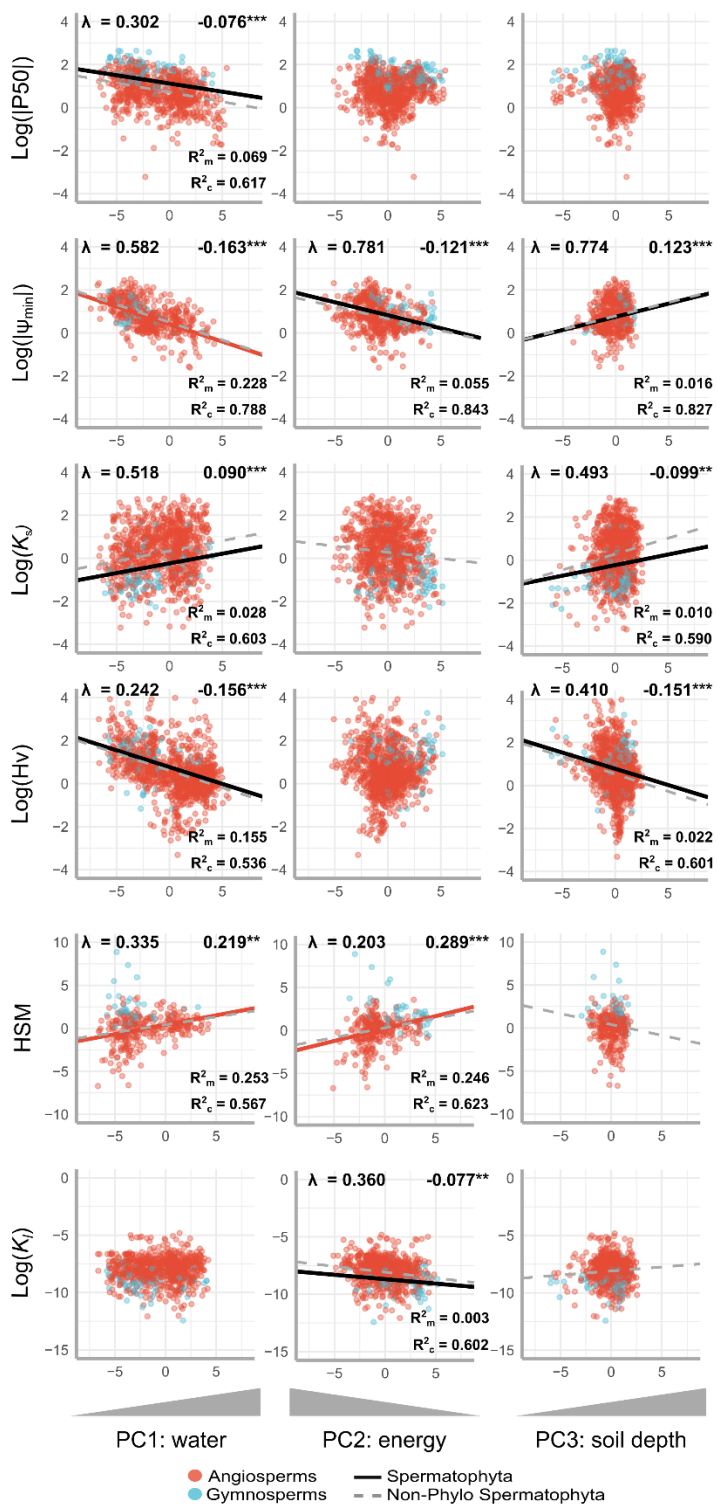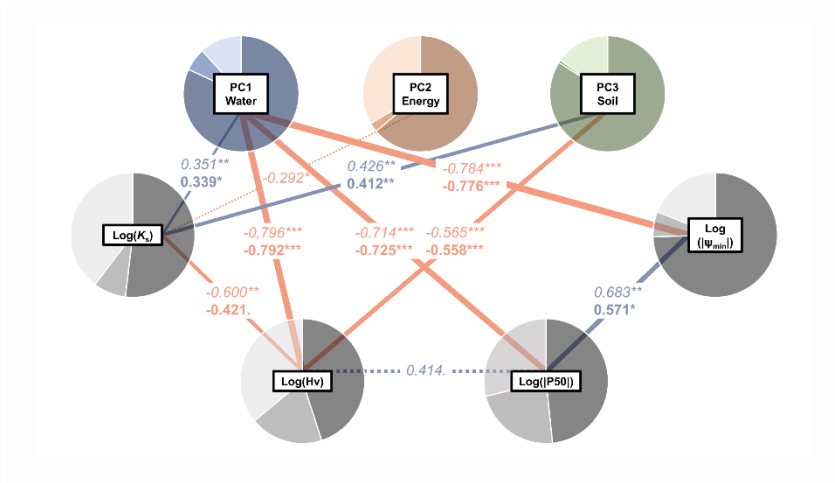
Supporting information

655 **Figure S1. Whittaker diagrams.**

656 Whittaker diagrams for all observations available (once matched with the phylogeny) and

657 observations used for each one of the evolutionary correlations calculation (which has been

658 restricted to those species with complete observations for the two traits and with genus-level

659 phylogenetic information available).

660
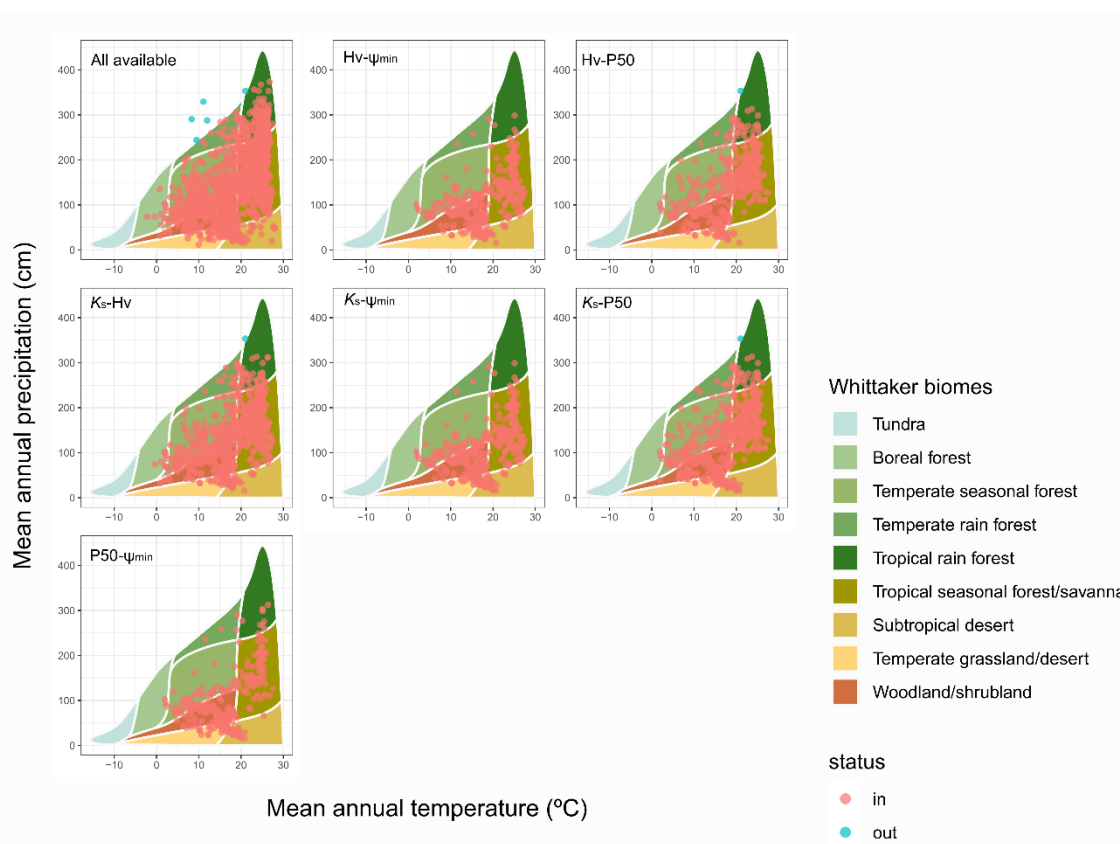
40

661 **Figure S2. Geographic distribution of the three main environmental principal components.**

662 Species-mean coordinates are plotted for each species coloured by their environmental principal

663 components mean values. Thus, some coordinates fall into the sea (presumably species present in

664 both the Palearctic and the Nearctic realms). However, note that environmental variables were

665 calculated for each occurrence of each species separately and then averaged to the species level.

666 PC1 (a) is mainly related to water availability variables, PC2 (b) to energy input and PC3 (b) to

667 soil depth (see Table S2 for a more concrete list of variables and their contribution to each of the

668 three principal component).

669
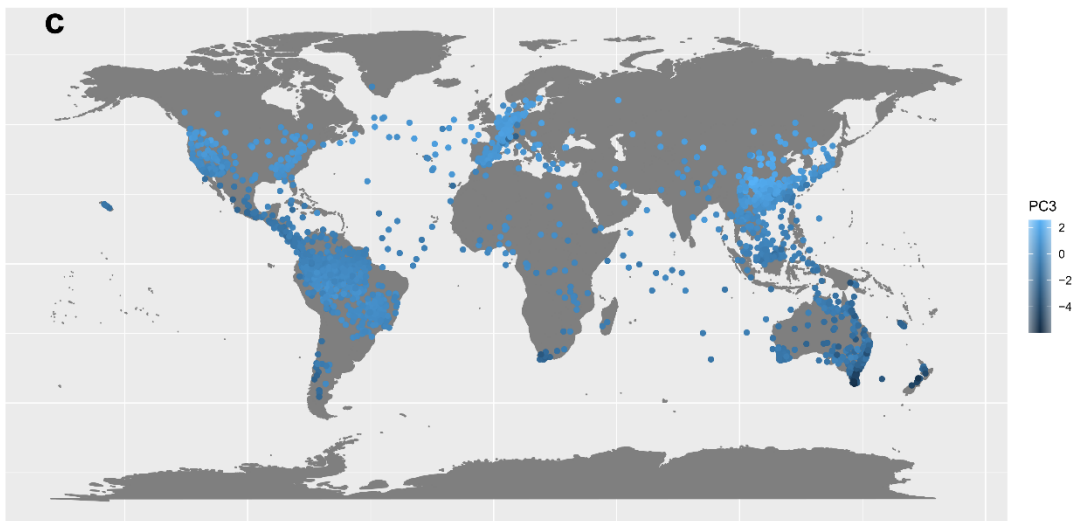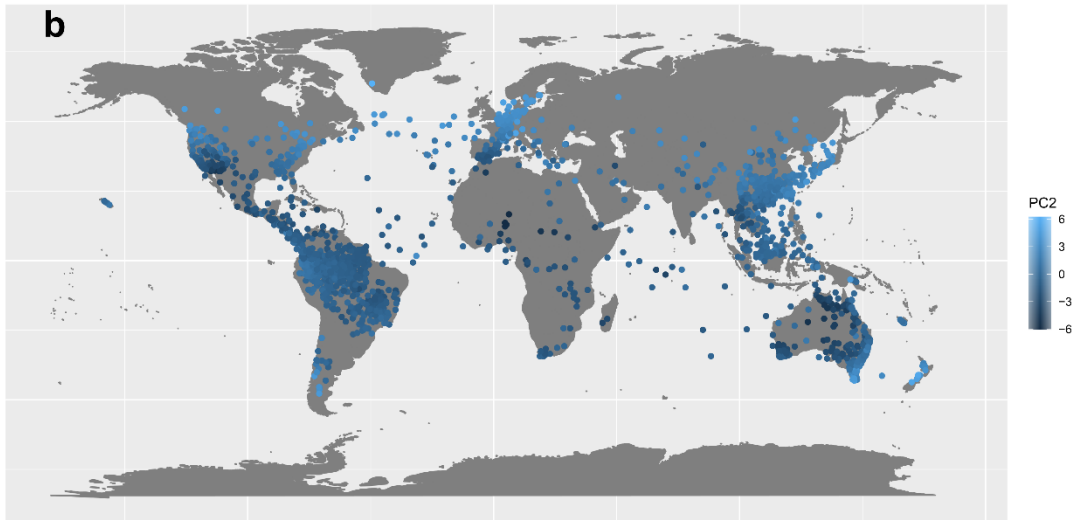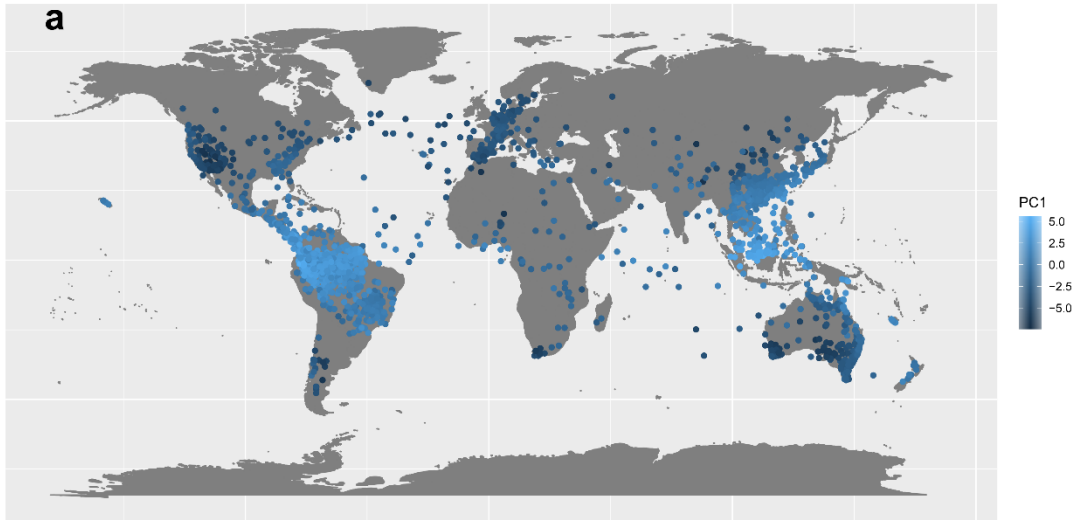
670 **Figure S3. PCA biplot environment-hydraulic relationships.**

671 PCA biplots showing the contributions of the 10 most important environmental variables to the

672 first two principal components, PC1 and PC2 (a) and to PC1 and PC3 (b), colouring species as

673 angiosperms (red circles) or gymnosperms (light blue triangles). Environmental variance

674 explained for each principal component is shown in percentage. log(TS): temperature seasonality

675 (log. transformed); pH: soil pH measured at 60 cm; VPD_{max}: maximum vapour pressure deficit;

676 T_{max}: mean of the monthly maximum temperatures; MAT: mean annual temperature; Clay: clay

677 content in percentage measured at 60cm, log(Wet P): Precipitation of the wettest month (log.

678 Transformed); AP: annual precipitation; AI: aridity index (which is actually a moisture index);

679 sqrt(DQ P): dry quarter precipitation (square root transformed); Soil depth: absolute depth to

680 bedrock, SWC: soil water content at 200cm, $Wind_{max}$: mean of the monthly maximum wind

681 velocity.

682

43
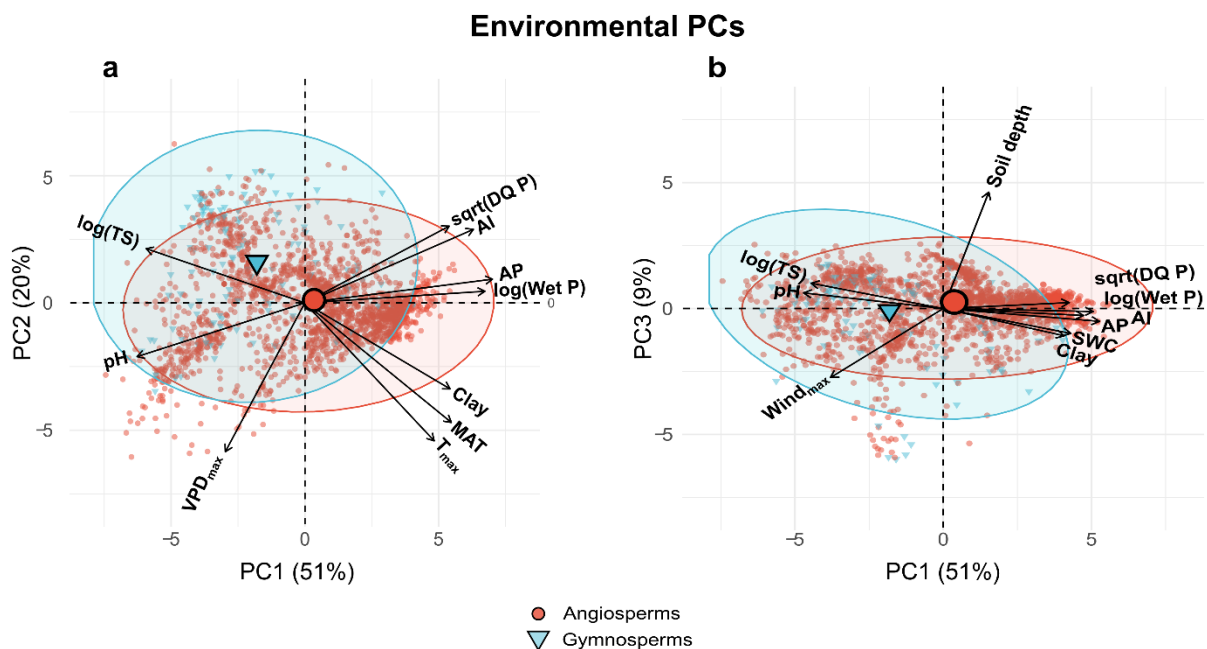
683 **Figure S4. Phylogenetic reconstruction of Hydraulic Safety Margin (HSM) and leaf-specific**

684 **hydraulic conductivity (log-transformed, log(K_l)) under a Brownian motion model of**

685 **evolution.**

686 Families with more than one genus are presented and some of the most important families are

687 highlighted in bold. Gymnosperm families are displayed in grey and angiosperm ones in black.

Hydraulic Safety Margin (HSM)
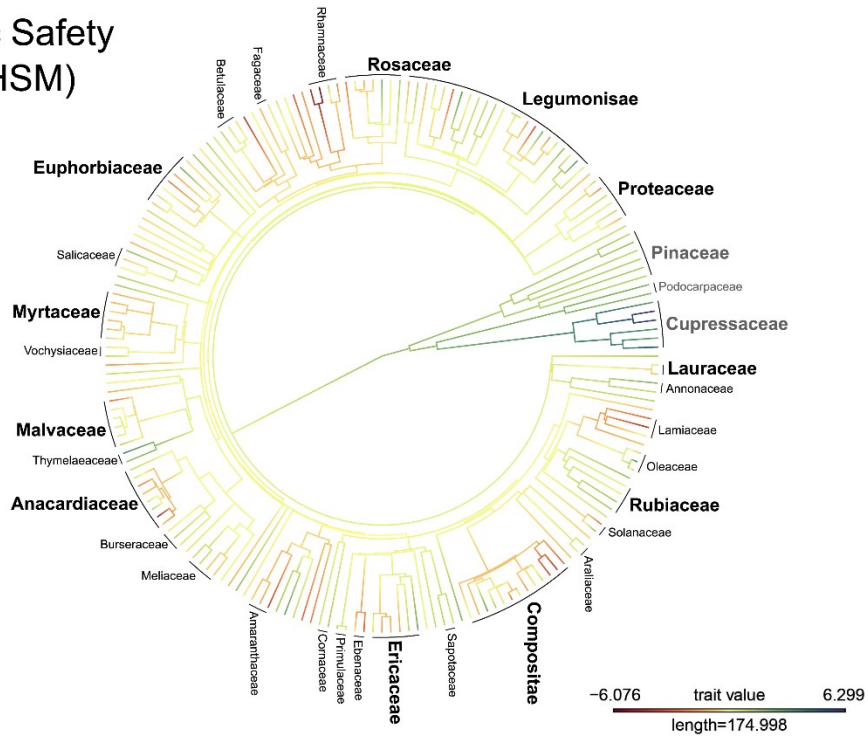
Leaf specific conductivity (log(K_l))

688

45
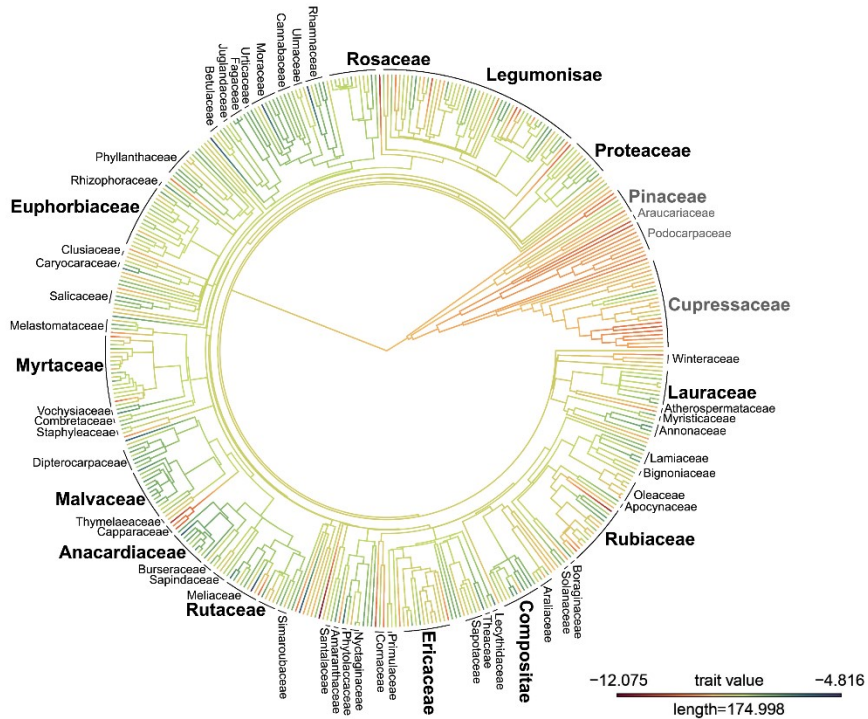
689 **Figure S5. Phylogenetic reconstruction of the three environmental principal components**

690 **under a Brownian motion model of evolution.**

691 Families with more than one genus are presented and some of the most important families are

692 highlighted in bold. Gymnosperm families are displayed in grey and angiosperm ones in black.

693 PC1 refer to the first environmental principal component, representing variation in water

694 availability and some related variables such as soil pH, soil clay content, soil water content and

695 temperature seasonality, with high values characterizing more humid locations with leached acidic

696 soils characteristic of tropical habitats. PC2 refer to the second environmental principal

697 component, representing variation in energy input, with high values characterizing low solar

698 irradiation, low maximum temperatures and low atmospheric water demand. PC3 refer to the third

699 environmental principal component, largely reflected by soil depth and, to a lower extent, wind

700 velocity, with high values indicating deeper soils with low sand content and low maximum wind

701 velocities.
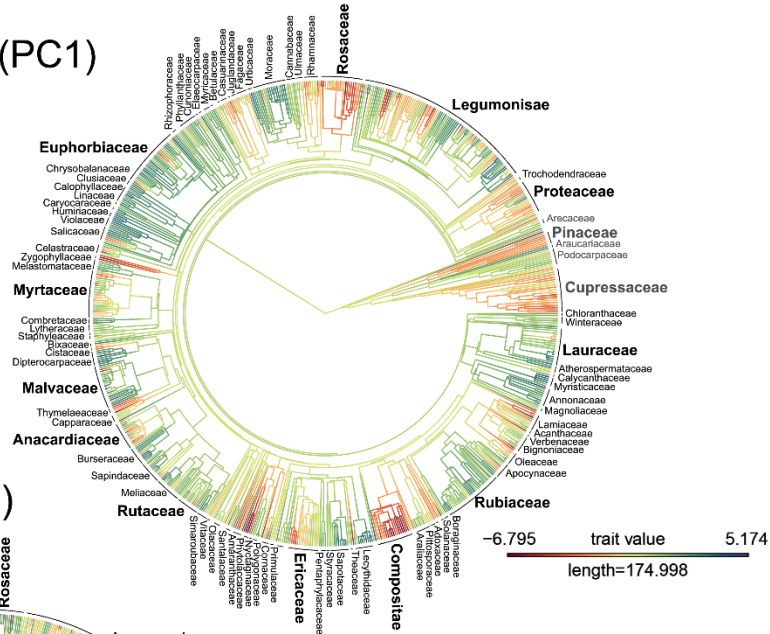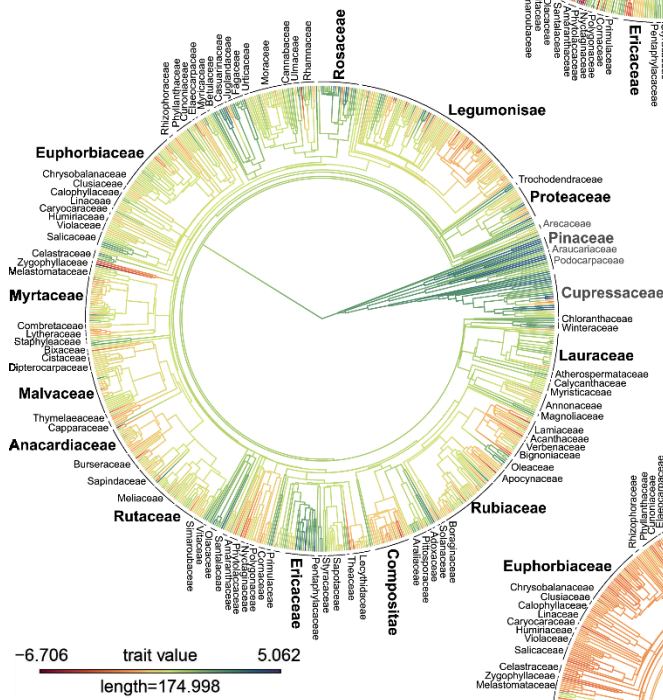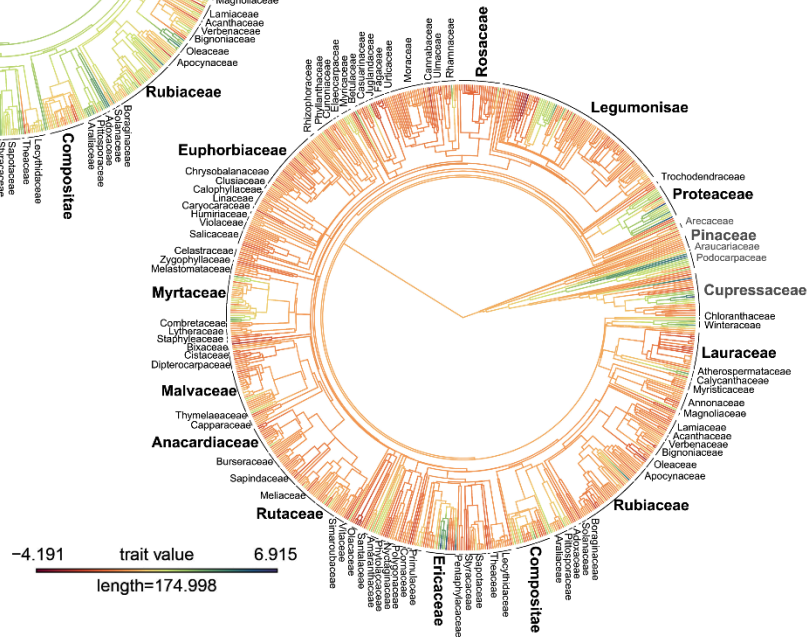
Figure S6. Evolutionary correlations when using the species-level phylogeny.

Evolutionary correlations between hydraulic traits and between traits and environmental variables (environmental variables represent orthogonal PC axes and as such are not correlated) using a species-level phylogeny. Lines represent significant evolutionary correlations (i.e., when the credible interval for the estimated correlation do not include zero), with the thickness of the line proportional to the strength of the correlation coefficient (also given on the same line). Light red lines represent negative relationships, dark blue one's indicate positive relationships. Significant correlations coefficients between traits when excluding environmental effects and evolutionary affiliation as fixed effects are shown in italics, and significant correlation coefficients between traits including environmental effects and evolutionary affiliation as fixed effects are shown in bold (in the case of the relationships between environmental axis and traits, only evolutionary affiliation was considered). Dashed line represents evolutionary correlation that became non-significant when environmental effects and major evolutionary affiliations were considered. Pie charts represent phylogenetic (dark) and intraspecific (light) variances reported in Appendix 2 (i.e., calculated using the maximum number of observations for each case). P-values are also displayed for each coefficient. Signif. codes: '***': $P < 0.001$; '**': $P < 0.01$; '*': $P < 0.05$ '.': $P < 0.1$ ' ': $P > 0.1$.

719
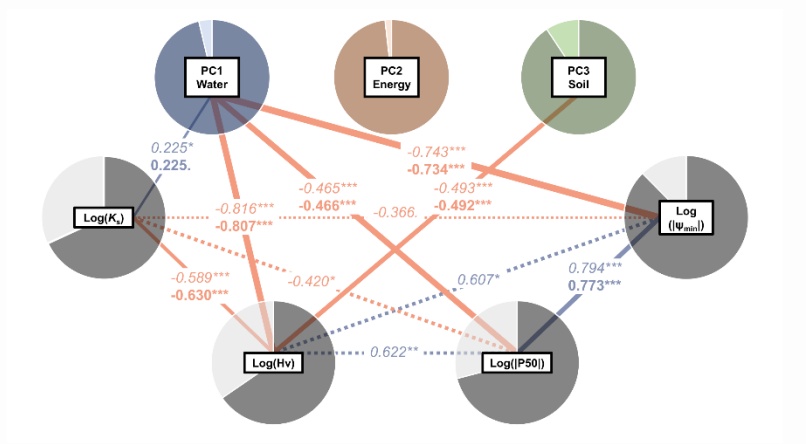
49

720 **Figure S7. Gymnosperms observations for the relationships between HSM and ψ$_{min}$ with**

721 **PC1 and the one between HSM and PC2**.

722 Species with HSM and ψ$_{min}$ data available are shown coloured by family. PC1 refers to the

723 environmental principal component mainly explained by water availability, PC2 refers to the

724 principal component mainly explained by decreasing energy input.
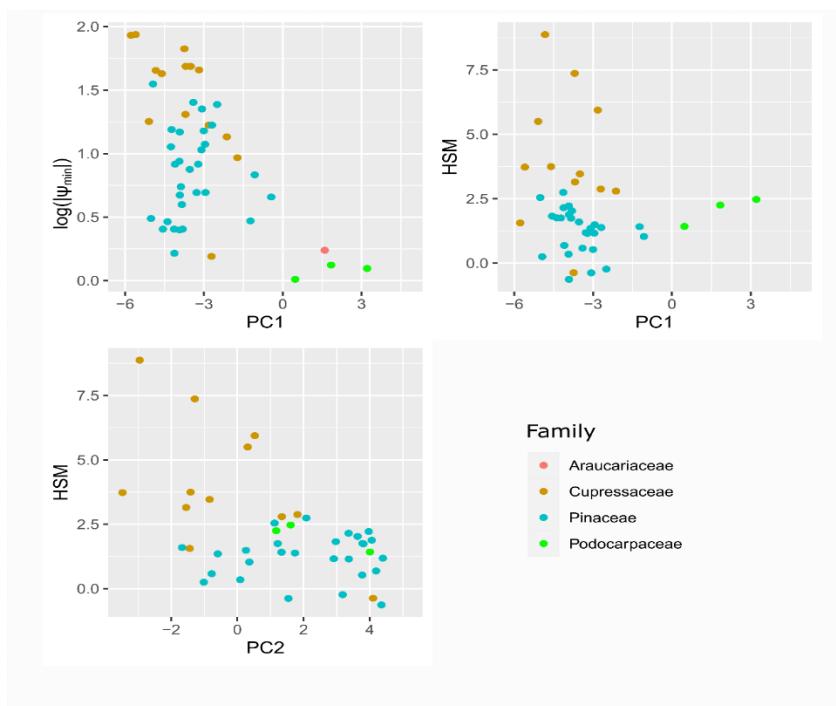
725

726 **Table S1. Number of observations variables abbreviation and transformations.**

727 Environmental variable and hydraulic traits nomenclature and number of whole dataset and major

728 evolutionary affiliation observations. In the "Transformation" column data transformations are

729 specified, when implemented.

Variable	Trasformation	Abbrebiation	Total observations	Angiosperms	Gymnosperms
Potential at the 50% loss of conductivity	Logaritmic of the absolute value	P50	894	771	123
Maximum stem-specific hydraulic conductivity	Logaritmic	K_s	1051	951	100
Leaf-specific hydraulic conductivity	Logaritmic	K_l	845	769	76
Huber value (sapwood area:leaf area ratio)	Logaritmic	Hv	1298	1223	75
Minimum water potential recorded	Logaritmic of the absolute value	ψ_{min}	553	505	48
Hydraulic Safety Margin (ψmin-P50)		HSM	336	294	42
Precipitation warmest quarter	Square root	sqrt(WQ P)	1937	1808	129
Precipitation wettest month	Logaritmic	log(Wet P)	1937	1808	129
Mean of the monthly maximum temperature		T_{max}	1937	1808	129
Temperature seasonality	Logaritmic	log(TS)	1937	1808	129
Annual precipitation		AP	1937	1808	129
Precipitation driest quarter	Square root	sqrt(DQ P)	1937	1808	129
Mean annual temperature		MAT	1937	1808	129
Aridity index (which is actually a moisture index)		AI	1937	1808	129
Solar radiation		srad	1937	1808	129
Mean of the monthly maximum wind velocity		$wind_{max}$	1937	1808	129
Maximum vapour pressure deficit		VPD_{max}	1937	1808	129
Absolute depth to bed rock		Soil depth	1937	1808	129
pH measured at 60cm		pH	1937	1808	129
Clay content in percentage measured at 60cm		Clay	1937	1808	129
Sand content in percentage measured at 60cm		Sand	1937	1808	129
Soil water content at 200cm		SWC	1937	1808	129

Table S2. Contribution of environmental variables to the three environmental principal components.

The highest contribution is highlighted for each variable. Sqrt(WQ P): Precipitation warmest quarter (square root transformed); log(Wet P): Precipitation wettest month (log. Transformed); T_{max}: Mean of the monthly maximum temperature; log(TS): Temperature seasonality (log. Transformed); AP: Annual precipitation; sqrt(DQ P): Precipitation driest quarter (square root Transformed); MAT: Mean annual temperature; AI: Aridity index (which is actually a moisture index); srad: Solar radiation; $Wind_{max}$: Mean of the monthly maximum wind velocity; VPD_{max}: Maximum vapour pressure deficit; Soil depth: Absolute depth to bedrock; pH: pH measured at 60cm; Clay: Clay content in percentage measured at 60cm; Sand: Sand content in percentage measured at 60cm; SWC: Soil water content at 200cm.

Variable	Contribution			Correlation		
	PC1	PC2	PC3	PC1	PC2	PC3
sqrt(WQ P)	**7.200**	2.273	0.125	0.766	0.269	0.042
log(Wet P)	**10.192**	0.121	0.031	0.912	0.062	-0.021
T_{max}	5.261	**16.947**	0.022	0.655	-0.734	-0.018
log(TS)	**7.906**	2.624	2.283	-0.803	0.289	0.181
AP	**11.069**	0.502	0.588	0.950	0.126	-0.092
sqrt(DQ P)	**6.551**	5.256	2.105	0.731	0.409	-0.174
MAT	6.749	**12.733**	0.041	0.742	-0.636	-0.024
AI	**8.932**	4.820	0.173	0.853	0.391	-0.050
srad	0.077	**20.291**	11.520	-0.079	-0.803	-0.406
$Wind_{max}$	5.767	3.142	**17.055**	-0.686	0.316	-0.495
VPD_{max}	1.986	**19.722**	0.920	-0.402	-0.792	0.115
Soil Depth	0.942	1.405	**48.430**	0.277	-0.211	0.833
pH	**8.843**	2.569	0.873	-0.849	-0.286	0.112
Clay	**6.636**	6.592	2.668	0.736	-0.458	-0.196
Sand	4.496	0.825	**10.945**	-0.606	-0.162	-0.396
SWC	**7.393**	0.178	2.220	0.776	0.075	-0.178

741 **Table S3. Reference table for all the models reported in the main text.**

742 All models were implemented with and without accounting for the phylogeny. In the fixed

743 structure column, variables to the right of the "~" symbol are response variables, those to the left

744 are predictors. Abbreviations: "env"(1): individual environmental principal component; env(3):

745 three main environmental principal components; trait: individual hydraulic trait; Affiliation: major

746 evolutionary affiliation (angiosperm or gymnosperm), "1" refer to the intercept.

Fixed structure	Description	Phylogeny used	Number of response variables	Results Ref.
env(1) ~ 1	Phylogenetic signal	Genus-level	Uni-response	Table 1, Fig. 4 (pie charts)
trait ~ 1		Genus-level	Uni-response	Table 1, Fig. 4 (pie charts)
trait ~ env(1)	Uni-response environment models	Genus-level	Uni-response	Fig. 4, Table S5
trait ~ env(1) + Affiliation		Genus-level	Uni-response	Fig. 4, Table S5
trait ~ env(1) * Affiliation		Genus-level	Uni-response	Fig. 4, Table S5
trait , env(1) ~ 1	Evolutionary correlations	Genus-level	Bi-response	Fig. 5, Table S6
trait , env(1) ~ 1 + Affiliation		Genus-level	Bi-response	Fig. 5, Table S6
trait , trait ~ 1		Genus-level	Bi-response	Fig. 5, Table S6
trait , trait ~ 1 + Affiliation		Genus-level	Bi-response	Fig. 5, Table S6
trait , trait ~ 1 + env(3)		Genus-level	Bi-response	Fig. 5, Table S6
trait , trait ~ 1 + env(3) + Affiliation		Genus-level	Bi-response	Fig. 5, Table S6

trait , trait ~ 1 + env(3) * Affiliation		Genus-level	Bi-response	Fig. 5, Table S6
env(1) ~ 1	Phylogenetic signal	Species-level	Uni-response	Appendix 2, Fig. S6
trait ~ 1		Species-level	Uni-response	Appendix 2, Fig. S6
trait , env(1) ~ -1	Evolutionary correlations	Species-level	Bi-response	Appendix 2, Fig. S6
trait , env(1) ~ -1 + Affiliation		Species-level	Bi-response	Appendix 2, Fig. S6
trait , trait ~ -1		Species-level	Bi-response	Appendix 2, Fig. S6
trait , trait ~ -1 + env(3) * Affiliation		Species-level	Bi-response	Appendix 2, Fig. S6

747

748 **Table S4. Non-phylogenetic model's variance partition.**

749 Mean non-phylogenetic inter-generic (γ) and non-phylogenetic intra-generic (ρ) variance in non-

750 phylogenetic models without fixed effects. Note that phylogenetic variance (λ) is 0, as the

751 phylogenetic effect was not considered.

variable	Phylogenetic (λ)	Inter-generic (γ)	Intra-generic (ρ)
HSM	0	0.490	0.510
Log(Hv)	0	0.514	0.486
Log(K_l)	0	0.280	0.720
Log(K_s)	0	0.459	0.541
Log($|\psi_{min}|$)	0	0.621	0.379
Log($|P50|$)	0	0.636	0.364
PC1	0	0.787	0.213
PC2	0	0.483	0.517
PC3	0	0.641	0.359

Table S5. Uni-response models description.

DICs and explained variances for phylogenetic and non-phylogenetic uni-response models. The fixed formula is shown in each case. DICs for the phylogenetic models are shown. "NP" refer to non-phylogenetic models (i.e., only including genus contingency as random effect) explained variances. R2c refer to the conditional and R2m refers to the marginal explained variances. Abbreviations: K_s: Xylem conductivity; P50: xylem resistance to embolism; Hv: sapwood allocation relative to leaf area; ψ_{min}: drought exposure, HSM: hydraulic safety margin; K_l: and sufficiency; PC1: water availability; PC2: energy input and PC3: soil depth; Affiliation: evolutionary affiliation (angiosperm or gymnosperm).

Fixed effects formula	DIC	R2m	R2c	NP R2m	NP R2c
HSM ~ 1	1181	0	0.612	0	0.49
HSM ~ PC1 * Affiliation	1133	0.253	0.657	0.301	0.554
HSM ~ PC1 + Affiliation	1138	0.211	0.647	0.268	0.535
HSM ~ PC1	1139	0.065	0.625	0.026	0.519
HSM ~ PC2 * Affiliation	1133	0.246	0.623	0.28	0.509
HSM ~ PC2 + Affiliation	1142	0.184	0.658	0.237	0.54
HSM ~ PC2	1143	0.035	0.619	0.031	0.495
HSM ~ PC3 * Affiliation	1146	0.172	0.624	0.23	0.542
HSM ~ PC3 + Affiliation	1147	0.176	0.634	0.235	0.541
HSM ~ PC3	1150	0.006	0.618	0.02	0.528
log_Hv ~ 1	3147	0	0.641	0	0.514
log_Hv ~ PC1 + Affiliation	3013	0.166	0.549	0.187	0.479
log_Hv ~ PC1	3013	0.155	0.536	0.184	0.477
log_Hv ~ PC1 * Affiliation	3014	0.168	0.551	0.188	0.478
log_Hv ~ PC2 * Affiliation	3058	0.028	0.662	0.014	0.51
log_Hv ~ PC2	3060	0.002	0.646	0.001	0.509
log_Hv ~ PC2 + Affiliation	3060	0.028	0.657	0.013	0.509
log_Hv ~ PC3 + Affiliation	3066	0.045	0.615	0.04	0.477
log_Hv ~ PC3	3066	0.022	0.601	0.032	0.48
log_Hv ~ PC3 * Affiliation	3068	0.045	0.614	0.043	0.475
log_K_l ~ 1	2348	0	0.47	0	0.28
log_K_l ~ PC1 * Affiliation	2250	0.067	0.482	0.077	0.299
log_K_l ~ PC1	2252	0.002	0.447	0.002	0.282
log_K_l ~ PC1 + Affiliation	2254	0.069	0.463	0.077	0.296

$\log\_K_l \sim$ PC2	2250	0.016	0.41	0.033	0.254
$\log\_K_l \sim$ PC2 * Affiliation	2251	0.089	0.439	0.093	0.283
$\log\_K_l \sim$ PC2 + Affiliation	2251	0.084	0.434	0.088	0.276
$\log\_K_l \sim$ PC3	2250	0.002	0.454	0.008	0.297
$\log\_K_l \sim$ PC3 + Affiliation	2252	0.072	0.462	0.077	0.304
$\log\_K_l \sim$ PC3 * Affiliation	2253	0.075	0.47	0.077	0.304
$\log\_K_s \sim 1$	2795	0	0.608	0	0.459
$\log\_K_s \sim \log\_Hv$	2079	0.116	0.614	0.181	0.494
$\log\_K_s \sim \log\_Hv$ * Affiliation	2081	0.166	0.64	0.23	0.506
$\log\_K_s \sim \log(|P50|)$	1581	0.041	0.634	0.074	0.499
$\log\_K_s \sim \log(|P50|)$ * Affiliation	1583	0.111	0.666	0.118	0.51
$\log\_K_s \sim$ PC1	2670	0.028	0.603	0.042	0.475
$\log\_K_s \sim$ PC1 + Affiliation	2670	0.084	0.631	0.089	0.479
$\log\_K_s \sim$ PC1 * Affiliation	2670	0.091	0.635	0.09	0.479
$\log\_K_s \sim$ PC2	2694	0.003	0.602	0.01	0.447
$\log\_K_s \sim$ PC2 + Affiliation	2694	0.057	0.623	0.055	0.453
$\log\_K_s \sim$ PC2 * Affiliation	2696	0.058	0.625	0.056	0.456
$\log\_K_s \sim$ PC3	2685	0.01	0.59	0.028	0.462
$\log\_K_s \sim$ PC3 + Affiliation	2685	0.063	0.618	0.069	0.462
$\log\_K_s \sim$ PC3 * Affiliation	2687	0.062	0.617	0.07	0.463
$\log(|\psi_{min}|) \sim 1$	828	0	0.812	0	0.621
$\log(|\psi_{min}|) \sim \log(|P50|)$	431	0.279	0.738	0.299	0.71
$\log(|\psi_{min}|) \sim \log(|P50|)$ * Affiliation	432	0.29	0.738	0.314	0.703
$\log(|\psi_{min}|) \sim$ PC1 * Affiliation	688	0.228	0.788	0.303	0.686
$\log(|\psi_{min}|) \sim$ PC1	692	0.211	0.763	0.302	0.679
$\log(|\psi_{min}|) \sim$ PC1 + Affiliation	692	0.229	0.781	0.302	0.68
$\log(|\psi_{min}|) \sim$ PC2 * Affiliation	724	0.099	0.854	0.107	0.692
$\log(|\psi_{min}|) \sim$ PC2	725	0.055	0.843	0.094	0.691
$\log(|\psi_{min}|) \sim$ PC2 + Affiliation	725	0.099	0.854	0.104	0.687
$\log(|\psi_{min}|) \sim$ PC3 + Affiliation	793	0.07	0.841	0.047	0.649
$\log(|\psi_{min}|) \sim$ PC3	793	0.016	0.827	0.036	0.644
$\log(|\psi_{min}|) \sim$ PC3 * Affiliation	795	0.072	0.841	0.051	0.65
$\log(|P50|) \sim 1$	1426	0	0.71	0	0.636
$\log(|P50|) \sim$ PC1 * Affiliation	1396	0.193	0.635	0.23	0.605
$\log(|P50|) \sim$ PC1	1397	0.069	0.617	0.097	0.588
$\log(|P50|) \sim$ PC1 + Affiliation	1397	0.194	0.636	0.231	0.606
$\log(|P50|) \sim$ PC2 * Affiliation	1402	0.116	0.725	0.148	0.635
$\log(|P50|) \sim$ PC2 + Affiliation	1403	0.108	0.719	0.141	0.631
$\log(|P50|) \sim$ PC2	1403	0.001	0.694	0.002	0.623
$\log(|P50|) \sim$ PC3 * Affiliation	1394	0.107	0.728	0.141	0.637
$\log(|P50|) \sim$ PC3 + Affiliation	1397	0.105	0.725	0.144	0.636

log(|P50|) ~ PC3	1397	0.003	0.699	0.002	0.628
PC1 ~ 1	6985	0	0.891	0	0.787
PC2 ~ 1	6723	0	0.697	0	0.483
PC3 ~ 1	4707	0	0.85	0	0.641

Table S6. Evolutionary correlations and DICs for bi-response models.

Mean of the evolutionary correlation (Cor), credible interval (lower and upper HDP) and p-value reported by bi-response models. The fixed formula is shown in each case. Models are ordered by DIC values (from lower to higher) for each set of nested models (same response variables). Statistically significant evolutionary correlations are highlighted in bold and marginally significant in italics. Abbreviations: K_s: Xylem conductivity; P50: xylem resistance to embolism; Hv: sapwood allocation relative to leaf area; ψ_{min}: drought exposure, HSM: hydraulic safety margin; K_l: and sufficiency; PC1: water availability; PC2: energy input and PC3: soil depth; Affiliation: evolutionary affiliation (angiosperm or gymnosperm).

Var. 1	Var. 2	Fixed formula	Cor	Lower HDP	Upper HDP	p-value	DIC
log(Hv)	log(|ψ_{min}|)	(log(Hv), log(|ψ_{min}|)) ~ 1 + (PC1 + PC2 + PC3) * :Affiliation	-0.094	-0.681	0.436	0.752	1403
log(Hv)	log(|ψ_{min}|)	(log(Hv), log(|ψ_{min}|)) ~ 1 + PC1 + PC2 + PC3	-0.100	-0.636	0.486	0.736	1403
log(Hv)	log(|ψ_{min}|)	(log(Hv), log(|ψ_{min}|)) ~ 1 + Affiliation + PC1 + PC2 + PC3	-0.117	-0.624	0.462	0.664	1404
log(Hv)	log(|ψ_{min}|)	(log(Hv), log(|ψ_{min}|)) ~ 1 + Affiliation	0.222	-0.405	0.801	0.494	1571
log(Hv)	log(|ψ_{min}|)	(log(Hv), log(|ψ_{min}|)) ~ 1	0.217	-0.405	0.798	0.509	1571
log(Hv)	**PC1**	**(log(Hv), PC1) ~ 1**	**-0.796**	**-0.913**	**-0.662**	**0.000**	**7475**
log(Hv)	**PC1**	**(log(Hv), PC1) ~ 1 + Affiliation**	**-0.792**	**-0.910**	**-0.657**	**0.000**	**7475**
log(Hv)	PC2	(log(Hv), PC2) ~ 1 + Affiliation	0.145	-0.160	0.462	0.397	7296
log(Hv)	PC2	(log(Hv), PC2) ~ 1	0.156	-0.141	0.473	0.363	7296
log(Hv)	**PC3**	**(log(Hv), PC3) ~ 1 + Affiliation**	**-0.558**	**-0.747**	**-0.363**	**0.000**	**5971**
log(Hv)	**PC3**	**(log(Hv), PC3) ~ 1**	**-0.565**	**-0.737**	**-0.367**	**0.000**	**5972**
log(K_s)	*log(Hv)*	*(log(K_s)_log(Hv)) ~ 1 + PC1 + PC2 + PC3*	*-0.423*	*-0.805*	*-0.016*	*0.077*	*3843*
log(K_s)	*log(Hv)*	*(log(K_s)_log(Hv)) ~ 1 + Affiliation + PC1 + PC2 + PC3*	*-0.423*	*-0.795*	*-0.005*	*0.079*	*3843*
log(K_s)	*log(Hv)*	*cbind(log_(K_s)_log(Hv)) ~ 1 + (PC1 + PC2 + PC3) * Affiliation*	*-0.421*	*-0.827*	*-0.012*	*0.085*	*3853*
log(K_s)	**log(Hv)**	**(log(K_s), log(Hv)) ~ 1**	**-0.600**	**-0.868**	**-0.271**	**0.008**	**4058**
log(K_s)	**log(Hv)**	**(log(K_s), log(Hv)) ~ 1 + Affiliation**	**-0.588**	**-0.879**	**-0.247**	**0.010**	**4059**
log(K_s)	log(|ψ_{min}|)	(log(K_s), log(|ψ_{min}|)) ~ 1 + (PC1 + PC2 + PC3) * Affiliation	0.019	-0.538	0.566	0.934	1571
log(K_s)	log(|ψ_{min}|)	(log(K_s), log(|ψ_{min}|)) ~ 1 + Affiliation + PC1 + PC2 + PC3	-0.013	-0.535	0.569	0.966	1572
log(K_s)	log(|ψ_{min}|)	(log(K_s), log(|ψ_{min}|)) ~ 1 + PC1 + PC2 + PC3	0.008	-0.512	0.555	0.970	1572

$\log(K_s)$	$\log(|\psi_{min}|)$	$(\log(K_s), \log(|\psi_{min}|)) \sim 1$	-0.080	-0.683	0.487	0.785	1768
$\log(K_s)$	$\log(|\psi_{min}|)$	$(\log(K_s), \log(|\psi_{min}|)) \sim 1 + \text{Affiliation}$	-0.066	-0.675	0.507	0.823	1768
$\log(K_s)$	$\log(|P50|)$	$(\log(K_s), \log(|P50|)) \sim 1 + \text{Affiliation} + PC1 + PC2 + PC3$	-0.046	-0.517	0.399	0.851	2489
$\log(K_s)$	$\log(|P50|)$	$(\log(K_s), \log(|P50|)) \sim 1 + PC1 + PC2 + PC3$	-0.098	-0.510	0.324	0.648	2489
$\log(K_s)$	$\log(|P50|)$	$(\log(K_s), \log(|P50|)) \sim 1 + (PC1 + PC2 + PC3) * \text{Affiliation}$	-0.019	-0.475	0.408	0.917	2495
$\log(K_s)$	$\log(|P50|)$	$(\log(K_s), \log(|P50|)) \sim 1$	-0.317	-0.665	0.055	0.114	2596
$\log(K_s)$	$\log(|P50|)$	$(\log(K_s), \log(|P50|)) \sim 1 + \text{Affiliation}$	-0.274	-0.639	0.165	0.211	2596
$\log(K_s)$	**PC1**	**$(\log(K_s), PC1) \sim 1 + \text{Affiliation}$**	**0.339**	**0.093**	**0.578**	**0.010**	**6343**
$\log(K_s)$	**PC1**	**$(\log(K_s), PC1) \sim 1$**	**0.351**	**0.110**	**0.594**	**0.009**	**6343**
$\log(K_s)$	PC2	$(\log(K_s), PC2) \sim 1 + \text{Affiliation}$	-0.275	-0.570	0.003	0.069	6315
$log(K_s)$	*PC2*	*$(log(K_s), PC2) \sim 1$*	*-0.292*	*-0.576*	*-0.007*	*0.048*	*6315*
$\log(K_s)$	**PC3**	**$(\log(K_s), PC3) \sim 1 + \text{Affiliation}$**	**0.412**	**0.144**	**0.683**	**0.008**	**5216**
$\log(K_s)$	**PC3**	**$(\log(K_s), PC3) \sim 1$**	**0.426**	**0.185**	**0.706**	**0.005**	**5216**
$\log(|\psi_{min}|)$	**PC1**	**$(\log(|\psi_{min}|), PC1) \sim 1 + \text{Affiliation}$**	**-0.776**	**-0.908**	**-0.624**	**0.000**	**2636**
$\log(|\psi_{min}|)$	**PC1**	**$(\log(|\psi_{min}|), PC1) \sim 1$**	**-0.784**	**-0.907**	**-0.620**	**0.000**	**2636**
$\log(|\psi_{min}|)$	PC2	$(\log(|\psi_{min}|), PC2) \sim 1$	-0.232	-0.566	0.129	0.214	2744
$\log(|\psi_{min}|)$	PC2	$(\log(|\psi_{min}|), PC2) \sim 1 + \text{Affiliation}$	-0.249	-0.594	0.124	0.195	2745
$\log(|\psi_{min}|)$	PC3	$(\log(|\psi_{min}|), PC3) \sim 1 + \text{Affiliation}$	0.115	-0.236	0.452	0.539	1916
$\log(|\psi_{min}|)$	PC3	$(\log(|\psi_{min}|), PC3) \sim 1$	0.126	-0.208	0.480	0.471	1917
$\log(|P50|)$	$\log(Hv)$	$(\log(|P50|), \log(Hv)) \sim 1 + PC1 + PC2 + PC3$	0.060	-0.423	0.507	0.818	1834
$\log(|P50|)$	$\log(Hv)$	$(\log(|P50|), \log(Hv)) \sim 1 + \text{Affiliation} + PC1 + PC2 + PC3$	0.061	-0.413	0.511	0.779	1835
$\log(|P50|)$	$\log(Hv)$	$(\log(|P50|), \log(Hv)) \sim 1 + (PC1 + PC2 + PC3) * \text{Affiliation}$	0.053	-0.404	0.531	0.831	1843
$log(|P50|)$	*$log(Hv)$*	*$(log(|P50|), log(Hv)) \sim 1$*	*0.414*	*0.052*	*0.790*	*0.070*	*1927*
$\log(|P50|)$	$\log(Hv)$	$(\log(|P50|), \log(Hv)) \sim 1 + \text{Affiliation}$	0.385	-0.043	0.777	0.121	1927
$\log(|P50|)$	**$\log(|\psi_{min}|)$**	**$(\log(|P50|), \log(|\psi_{min}|)) \sim 1 + (PC1 + PC2 + PC3) * \text{Affiliation}$**	**0.571**	**0.213**	**0.860**	**0.015**	**745**
$\log(|P50|)$	**$\log(|\psi_{min}|)$**	**$(\log(|P50|), \log(|\psi_{min}|)) \sim 1 + \text{Affiliation} + PC1 + PC2 + PC3$**	**0.552**	**0.168**	**0.863**	**0.030**	**751**
$\log(|P50|)$	**$\log(|\psi_{min}|)$**	**$(\log(|P50|), \log(|\psi_{min}|)) \sim 1 + PC1 + PC2 + PC3$**	**0.556**	**0.168**	**0.833**	**0.015**	**751**
$\log(|P50|)$	**$\log(|\psi_{min}|)$**	**$(\log(|P50|), \log(|\psi_{min}|)) \sim 1 + \text{Affiliation}$**	**0.702**	**0.428**	**0.917**	**0.000**	**834**
$\log(|P50|)$	**$\log(|\psi_{min}|)$**	**$(\log(|P50|), \log(|\psi_{min}|)) \sim 1$**	**0.683**	**0.386**	**0.914**	**0.006**	**834**
$\log(|P50|)$	**PC1**	**$(\log(|P50|), PC1) \sim 1 + \text{Affiliation}$**	**-0.725**	**-0.885**	**-0.537**	**0.000**	**4476**
$\log(|P50|)$	**PC1**	**$(\log(|P50|), PC1) \sim 1$**	**-0.714**	**-0.875**	**-0.524**	**0.000**	**4477**
$\log(|P50|)$	PC2	$(\log(|P50|), PC2) \sim 1$	0.050	-0.316	0.460	0.803	4487
$\log(|P50|)$	PC2	$(\log(|P50|), PC2) \sim 1 + \text{Affiliation}$	0.015	-0.344	0.400	0.978	4488
$\log(|P50|)$	PC3	$(\log(|P50|), PC3) \sim 1 + \text{Affiliation}$	-0.110	-0.456	0.208	0.570	3677
$\log(|P50|)$	PC3	$(\log(|P50|), PC3) \sim 1$	-0.097	-0.426	0.229	0.573	3678

770

59

Appendix S1. Supplementary methods.

Phylogenetic mixed model description

Phylogenetic mixed models are commonly used in quantitative genetics (the so called "animal" model), being useful for comparative analyses as they allow to incorporate a range of variance structures for the random effects, including shared ancestry through a phylogeny (Housworth *et al.* 2004). The general model structure is defined as follows:

$$y = \mu + \beta x + p + g + e \tag{1}$$

Were μ is the grand mean, interpreted as the root ancestor state, β is the slope for the covariate x (fixed effect, in green), p and g are the variability caused by the genus-level phylogeny and the genus contingency effects (random effects, in red), and e is the residual error (Housworth *et al.* 2004; Villemereuil & Nakagawa 2014). Both fixed (β) and random (r, which is $p + g$) effects and the residuals (e) are expected to come from a multivariate normal distribution as it follows:

$$\begin{bmatrix} \beta \\ r \\ e \end{bmatrix} \sim N \left(\begin{bmatrix} \beta_0 \\ 0 \\ 0 \end{bmatrix}, \begin{bmatrix} B & 0 & 0 \\ 0 & G & 0 \\ 0 & 0 & R \end{bmatrix} \right) \tag{2}$$

Where β is the fixed effect parameter to estimate, β_0 is the prior means for the fixed effects with prior (co)variance matrix B, and G and R are the expected (co)variances of the random effects and the residuals respectively (Hadfield 2010; Hadfield & Nakagawa 2010). G and R are unknown, and must be estimated from the data by assuming they are structured in a way that can be parametrized by few parameters, as it has been exemplified below for the G case:

$$G = \begin{bmatrix} V_{G_1} \otimes A_{G_1} & 0 \\ 0 & V_{G_2} \otimes A_{G_2} \end{bmatrix} \tag{3}$$

Were the (co)variance matrices (V) are matrices with one parameter to be estimated per response

791   variable and the structured matrices (A) refer to the phylogenetic structure (A_{G1}) and genus

792   contingency (A_{G2}). The Kronecker product ($\otimes$) allows for possible dependence between random

793   effects (Hadfield 2010; Hadfield & Nakagawa 2010).

794   In multi-response models, the (co)variance matrix of the previous equation is reformulated

795   including the covariance estimates in the off-diagonal and the respective variances in the diagonal

796   as follows:

797
$$V_{G1} = \begin{bmatrix} \sigma^2_{u_1} & \sigma_{u_1,u_2} \\ \sigma_{u_2,u_1} & \sigma^2_{u_2} \end{bmatrix} \tag{4}$$

798   Where σ^2_{u1} is the variance for the first response variable (V_1) and σ^2_{u2} the variance for the second

799   response variable (V_2), while $\sigma_{u1,u2}$ and $\sigma_{u2,u1}$ are the same covariance estimate (C).

800   *Phylogenetic indexes calculation*

801   The phylogenetic signal or phylogenetic heritability it is calculated as follows (Villemereuil &

802   Nakagawa 2014):

803
$$\lambda = \frac{\sigma^2_p}{\sigma^2_p + \sigma^2_g + \sigma^2_e} \tag{5}$$

804   Where σ^2_P is the variance of the phylogenetic effect (V_{G1}), σ^2_g is the variance of the cross-genus

805   effect (V_{G2}) and σ^2_e is the residual error (Villemereuil & Nakagawa 2014). Cross-genera variance

806   (i.e. non-phylogenetic variation among genera or genus lability) has been calculated as follows:

807
$$\gamma = \frac{\sigma^2_g}{\sigma^2_p + \sigma^2_g + \sigma^2_e} \tag{6}$$

808   And finally, intra-genus variability including measurement error has been calculated as follows:

809
$$\rho = \frac{\sigma^2_e}{\sigma^2_p + \sigma^2_g + \sigma^2_e} \tag{7}$$

810   Note also that $\gamma + \rho + \lambda = 1$ (Housworth *et al.* 2004). The three indexes were calculated for the

811   whole Markov chain random effects and residual samples (once burned and thinned), so the output

812   is a statistical distribution from which the mean and 95% credible intervals can be calculated.

813   *Phylogenetic covariation calculation*

814   From the phylogenetic variances and covariance in equation 4, the evolutionary correlation

815   between response variables can be calculated as follows (Villemereuil 2012):

816   $$r_{ev} = \frac{\sigma_{u_2,u_1}}{\sqrt{\sigma_{u_1}^2 \cdot \sigma_{u_2}^2}} \tag{8}$$

817   *Model specifications*

818   "MCMCglmm" implements a Bayesian approach, estimating the posterior distribution of

819   parameters, from which 95% credible intervals can be obtained (Hadfield 2010). We set

820   independent normal prior distributions for fixed effects and non-informative Inverse-Gamma prior

821   distributions for random effects and residual variances (Villemereuil & Nakagawa 2014). Less

822   informative expanded priors were also used, and highly similar results were obtained.

823   Uni-response models random effects variance priors were set as V = 1, nu = 0.002. For bi-response

824   models, the random effects variances priors were set as V = diag(2)/2, nu = 2. To achieve

825   convergence, each model was run for 8,000,000 iterations with a 1,000,000 burn-in and a thinning

826   interval of 4,000, reaching an effective sample size between 1,000 and 2,000 in all estimated

827   parameters. When models did not converge, we increased the number of iterations until

828   convergence were achieved. Thinning intervals and the final number of iterations were

829   progressively increased until autocorrelations between samples were found to be <0.1.

830   Convergence of all models was assessed by plots of chain mixing and by the Heidenberg stationary

831   test as a diagnostic. All reported models had a low degree of autocorrelation between iterations

832   and passed the convergence diagnostic, both for fixed and random effects (i.e., the sampled chains

833   were stationary).

834   *Literature cited*

835   Hadfield, J.D. (2010). MCMCglmm for R. *J. Stat. Softw.*, 33.

836   Hadfield, J.D. & Nakagawa, S. (2010). General quantitative genetic methods for comparative

837   biology: Phylogenies, taxonomies and multi-trait models for continuous and categorical

838   characters. *J. Evol. Biol.*, 23, 494–508.

839   Housworth, E.A., Martins, E.P. & Lynch, M. (2004). The Phylogenetic Mixed Model. *Am. Nat.*,

840   163, 84–96.

841   Villemereuil, P. (2012). How to use the MCMCglmm R package.

842   Villemereuil, P. & Nakagawa, S. (2014). General Quantitative Genetic Methods for Comparative

843   Biology. In: (*Modern Phylogenetic Comparative Methods and Their Application in*

844   *Evolutionary Biology: Concepts and Practice*), {[Garamszegi, L.Z.]}. Springer, New York,

845   USA. 287-303.

846   **Appendix S2. Species-level phylogenetic analyses.**

847   Species-level phylogeny was obtained by pruning the phylogenetic tree reported by Smith &

848   Brown (2018) available in the R package "v.PhyloMaker" (Jin & Qian 2019) by using the "ape"

849   R package (Paradis & Schliep 2018) only keeping species with hydraulic data available in each

850   case, obtaining the same number of observations compared to the genus-level analyses. Some bi-

851   response models implemented using the genus-level phylogeny where also conducted using the

852   species-level phylogeny. As we had only one value per specie, no extra random effect was

853   included, so variance partition was reduced to phylogenetic signal calculation.

854 *Phylogenetic signal results*

855 Variance partitioning for the six hydraulic traits and three environmental principal components

856 related to water availability (PC1), energy input (PC2) and soil depth (PC3). Legend: N: number

857 of species used in each case (for which both phylogenetic and hydraulic data were available),

858 phylogenetic variance (phylogenetic signal, λ) and non-phylogenetic intraspecific variance plus

859 measurement error (ρ). Mean and lower and upper 95% credible intervals (HDP) are shown for

860 each component.

variable	N	λ	λ lower HPD	λ upper HPD	ρ	ρ lower HDP	ρ Upper HDP
HSM	195	0.456	0.228	0.680	0.544	0.320	0.772
Log(Hv)	842	0.654	0.539	0.774	0.346	0.226	0.461
Log(K_l)	616	0.610	0.456	0.753	0.390	0.247	0.544
Log(K_s)	763	0.681	0.569	0.792	0.319	0.208	0.431
Log($|\psi_{min}|$)	358	0.876	0.799	0.940	0.124	0.060	0.201
log_negP50	693	0.709	0.594	0.817	0.291	0.183	0.406
PC1	1329	0.963	0.951	0.975	0.037	0.025	0.049
PC2	1329	0.845	0.796	0.889	0.155	0.111	0.204
PC3	1329	0.907	0.882	0.934	0.093	0.066	0.118

861

862 *Evolutionary correlations results*

863 Mean of the evolutionary correlation (Cor), credible interval (lower and upper HDP) and p-value

864 reported by bi-response models. Statistically significant evolutionary correlations are highlighted

865 in bold and marginally significant in italics. In the fixed structure column, variables to the right of

866 the "~" symbol are response variables, those to the left are predictors. Abbreviations: "env"(1):

867 individual environmental principal component; env(3): three main environmental principal

868 components; trait: individual hydraulic trait; Affiliation: major evolutionary affiliation

869 (angiosperm or gymnosperm).

Fixed structure	Var. 1	Var. 2	Cor	Lower HDP	Upper HDP	p-value
trait, trait ~ 1 + env(3) * Affiliation	log(Hv)	log(ψ_{min})	0.134	-0.365	0.695	0.641
trait, trait ~ 1	**log(Hv)**	**log(ψ_{min})**	**0.607**	**0.261**	**0.915**	**0.014**
trait, env(1) ~ 1	**log(Hv)**	**PC1**	**-0.807**	**-0.908**	**-0.699**	**0.000**
trait, env(1) ~ 1 + Affiliation	**log(Hv)**	**PC1**	**-0.816**	**-0.922**	**-0.714**	**0.000**
trait, env(1) ~ 1	log(Hv)	PC2	-0.090	-0.334	0.191	0.495
trait, env(1) ~ 1 + Affiliation	log(Hv)	PC2	-0.092	-0.376	0.164	0.501
trait, env(1) ~ 1 + Affiliation	**log(Hv)**	**PC3**	**-0.492**	**-0.689**	**-0.304**	**0.000**
trait, env(1) ~ 1	**log(Hv)**	**PC3**	**-0.493**	**-0.691**	**-0.304**	**0.000**
trait, trait ~ 1 + env(3) * Affiliation	**log(K_s)**	**log(Hv)**	**-0.630**	**-0.851**	**-0.359**	**0.000**
trait, trait ~ 1	**log(K_s)**	**log(Hv)**	**-0.589**	**-0.815**	**-0.348**	**0.000**
trait, trait ~ -1 + env(3) * Affiliation	log(K_s)	log(ψ_{min})	-0.217	-0.663	0.226	0.349
trait, trait ~ 1	*log(K_s)*	*log(ψ_{min})*	*-0.366*	*-0.703*	*0.012*	*0.090*
trait, trait ~ -1 + env(3) * Affiliation	log(K_s)	log(|P50|)	-0.236	-0.579	0.172	0.223
trait, trait ~ 1	**log(K_s)**	**log(|P50|)**	**-0.420**	**-0.674**	**-0.104**	**0.015**
trait, env(1) ~ 1	**log(K_s)**	**PC1**	**0.225**	**0.000**	**0.421**	**0.043**
trait, env(1) ~ 1 + Affiliation	*log(K_s)*	*PC1*	*0.225*	*0.006*	*0.452*	*0.067*
trait, env(1) ~ 1 + Affiliation	log(K_s)	PC2	-0.185	-0.434	0.065	0.160
trait, env(1) ~ 1	log(K_s)	PC2	-0.196	-0.439	0.092	0.155
trait, env(1) ~ 1 + Affiliation	log(K_s)	PC3	0.106	-0.132	0.350	0.395
trait, env(1) ~ 1	log(K_s)	PC3	0.105	-0.147	0.338	0.423
trait, env(1) ~ 1 + Affiliation	**log(ψ_{min})**	**PC1**	**-0.734**	**-0.861**	**-0.599**	**0.000**
trait, env(1) ~ 1	**log(ψ_{min})**	**PC1**	**-0.743**	**-0.868**	**-0.590**	**0.000**
trait, env(1) ~ 1 + Affiliation	log(ψ_{min})	PC2	-0.266	-0.573	0.041	0.127
trait, env(1) ~ 1	log(ψ_{min})	PC2	-0.254	-0.567	0.040	0.118
trait, env(1) ~ 1 + Affiliation	log(ψ_{min})	PC3	0.215	-0.032	0.462	0.101

trait, env(1) ~ 1	*log(|ψ$_{min}$|)*	*PC3*	*0.223*	*-0.032*	*0.453*	*0.097*
trait, trait ~ -1 + env * Affiliation	log(|P50|)	log(Hv)	0.211	-0.256	0.663	0.429
trait, trait ~ 1	**log(|P50|)**	**log(Hv)**	**0.622**	**0.370**	**0.839**	**0.001**
trait, trait ~ -1 + env(3) * Affiliation	**log(|P50|)**	**log(|ψ$_{min}$|)**	**0.773**	**0.582**	**0.926**	**0.000**
trait, env(1) ~ 1	**log(|P50|)**	**log(|ψ$_{min}$|)**	**0.794**	**0.636**	**0.923**	**0.000**
trait, env(1) ~ 1 + Affiliation	**log(|P50|)**	**PC1**	**-0.466**	**-0.658**	**-0.254**	**0.000**
trait, env(1) ~ 1	**log(|P50|)**	**PC1**	**-0.465**	**-0.661**	**-0.257**	**0.000**
trait, env(1) ~ 1 + Affiliation	log(|P50|)	PC2	0.022	-0.250	0.305	0.902
trait, env(1) ~ 1	log(|P50|)	PC2	0.032	-0.225	0.343	0.837
trait, env(1) ~ 1 + Affiliation	log(|P50|)	PC3	-0.147	-0.417	0.102	0.262
trait, env(1) ~ 1	log(|P50|)	PC3	-0.144	-0.390	0.118	0.279

870

Literature cited

872 Jin, Y., & Qian, H. (2019). V.PhyloMaker: an R package that can generate very large phylogenies for vascular plants. *Ecography*, 42(8), 1353–1359.

874 Paradis, E., & Schliep, K. (2018). ape 5.0: an environment for modern phylogenetics and evolutionary analyses in R. *Bioinformatics* 35: 526-528.

876 Smith, S. A., & Brown, J. W. (2018). Constructing a broadly inclusive seed plant phylogeny. *Am. J. Bot.*, 105(3), 302–314.

878 **Appendix S3. Evolutionary correlations reported by genus-level phylogenetic models using**

879 **observations available for the species-level phylogeny and evolutionary correlations**

880 **reported by species-level phylogeny pruned at the genus level.**

881 For bivariate models including two traits as response variable, only models without fixed effects

882 and models including the three environmental components and its interaction with major

883 evolutionary affiliation (angiosperm or gymnosperm) were implemented.

884 Significant evolutionary correlations (i.e., when the credible interval for the estimated correlation

885 do not include zero) reported by models using a genus-level phylogeny including only observations

886 available for the species-level phylogenetic analyses to check for effects of the different species

887 coverage between phylogenies. Mean of the evolutionary correlation (Cor), credible interval

888 (lower and upper HDP) and p-value reported by bi-response models. In the fixed structure column,

889 variables to the right of the "~" symbol are response variables, those to the left are predictors.

890 Abbreviations: "env"(1): individual environmental principal component; env(3): three main

891 environmental principal components; trait: individual hydraulic trait; Affiliation: major

892 evolutionary affiliation (angiosperm or gymnosperm).

Fixed structure	var1	var2	Cor	Lower HDP	Upper HDP	p-value
trait, env(1) ~ 1 + Affiliation	log(Hv)	PC1	-0.779	-0.926	-0.634	0.000
trait, env(1) ~ 1	log(Hv)	PC1	-0.787	-0.921	-0.647	0.000
trait, env(1) ~ 1 + Affiliation	log(Hv)	PC3	-0.499	-0.749	-0.250	0.001
trait, env(1) ~ 1	log(Hv)	PC3	-0.510	-0.749	-0.260	0.001
trait, trait ~ 1	log(K_s)	log(Hv)	-0.501	-0.850	-0.101	0.049
trait, trait ~ 1 + env(3) * Affiliation	log(K_s)	log(Hv)	-0.603	-0.861	-0.297	0.003
trait, trait ~ 1	log(K_s)	log(|P50|)	-0.394	-0.709	-0.022	0.054
trait, env(1) ~ 1 + Affiliation	log(K_s)	PC2	-0.316	-0.602	-0.011	0.049
trait, env(1) ~ 1	log(K_s)	PC2	-0.341	-0.618	-0.056	0.024
trait, env(1) ~ 1 + Affiliation	log(K_s)	PC3	0.350	0.045	0.633	0.031
trait, env(1) ~ 1	log(K_s)	PC3	0.355	0.065	0.651	0.021
trait, env(1) ~ 1 + Affiliation	log($|\psi_{min}|$)	PC1	-0.779	-0.926	-0.623	0.000

Fixed structure	var1	var2	Cor	Lower HDP	Upper HDP	p-value
trait, env(1) ~ 1	$\log(|\psi_{min}|)$	PC1	-0.783	-0.928	-0.621	0.000
trait, trait ~1	$\log(|P50|)$	$\log(Hv)$	0.495	0.126	0.816	0.014
trait, trait ~ 1	$\log(|P50|)$	$\log(|\psi_{min}|)$	0.485	0.065	0.836	0.054
trait, trait ~ 1 +env(3) * Affiliation	$\log(|P50|)$	$\log(|\psi_{min}|)$	0.598	0.233	0.888	0.008
trait, env(1) ~ 1 + Affiliation	$\log(|P50|)$	PC1	-0.628	-0.863	-0.394	0.000
trait, env(1) ~ 1	$\log(|P50|)$	PC1	-0.618	-0.831	-0.374	0.001

893

894 Significant evolutionary correlations (i.e., when the credible interval for the estimated correlation

895 do not include zero) reported by models using a species-level phylogeny pruned at genus-level to

896 check for effects of differences in the topology between phylogenies. Mean of the evolutionary

897 correlation (Cor), credible interval (lower and upper HDP) and p-value reported by bi-response

898 models. In the fixed structure column, variables to the right of the "~" symbol are response

899 variables, those to the left are predictors. Abbreviations: "env"(1): individual environmental

900 principal component; env(3): three main environmental principal components; trait: individual

901 hydraulic trait; Affiliation: major evolutionary affiliation (angiosperm or gymnosperm).

Fixed structure	var1	var2	Cor	Lower HDP	Upper HDP	p-value
trait, env(1) ~ 1 + Affiliation	$\log(Hv)$	PC1	-0.817	-0.924	-0.685	0.000
trait, env(1) ~ 1	$\log(Hv)$	PC1	-0.824	-0.936	-0.696	0.000
trait, env(1) ~ 1 + Affiliation	$\log(Hv)$	PC3	-0.439	-0.705	-0.158	0.008
trait, env(1) ~ 1	$\log(Hv)$	PC3	-0.451	-0.711	-0.159	0.012
trait, trait ~ 1	$\log(K_s)$	$\log(Hv)$	-0.535	-0.844	-0.178	0.018
trait, trait ~ 1 + env(3) * Affiliation	$\log(K_s)$	$\log(Hv)$	-0.626	-0.877	-0.330	0.002
trait, trait ~ 1	$\log(K_s)$	$\log(|P50|)$	-0.398	-0.749	-0.016	0.069
trait, env(1) ~ 1 + Affiliation	$\log(K_s)$	PC2	-0.326	-0.626	-0.013	0.046
trait, env(1) ~ 1	$\log(K_s)$	PC2	-0.332	-0.688	-0.037	0.068
trait, env(1) ~ 1	$\log(K_s)$	PC3	0.334	0.005	0.647	0.045
trait, env(1) ~ 1 + Affiliation	$\log(|\psi_{min}|)$	PC1	-0.774	-0.924	-0.614	0.000
trait, env(1) ~ 1	$\log(|\psi_{min}|)$	PC1	-0.783	-0.933	-0.619	0.000
trait, trait ~1	$\log(|P50|)$	$\log(Hv)$	0.505	0.131	0.814	0.024
trait, trait ~ 1	$\log(|P50|)$	$\log(|\psi_{min}|)$	0.493	0.066	0.858	0.054
trait, trait ~ 1 +env(3) * Affiliation	$\log(|P50|)$	$\log(|\psi_{min}|)$	0.591	0.177	0.906	0.034
trait, env(1) ~ 1 + Affiliation	$\log(|P50|)$	PC1	-0.609	-0.856	-0.349	0.001
trait, env(1) ~ 1	$\log(|P50|)$	PC1	-0.595	-0.831	-0.342	0.001

902